

The co-editor and referee's comments are presented followed by our responses in blue.

Co-Editor :

Dear Authors,

collecting the comments of the three different reviewers, it still remains a different task to give a recommendation for this manuscript. Overall, the manuscript provides important and interesting material, with which there is nothing wrong, but it provides just too much information, presented in a very descriptive way ("a work summary, rather than a synthesized scientific paper", as quoted by a reviewer). Therefore, I'm afraid that a reader will lose its interest when struggling through e.g. all the descriptions of the differences seen in the figures of global IWV means and trends. And this would really be a pity, given the workload put in the analysis. So, I follow the referee #1 that the manuscript is still too long and should be considerably shortened. Please follow the general comment of this referee regarding Sections 4 and 5. I will also give some specific indications on which parts could be significantly shortened later on. But furthermore, I would also go through your manuscript once more and ask yourself at every sentence the questions: "Is this sentence really necessary? Does it provide new information? Has the information provided not already been given at another location in the manuscript?"

Secondly, I also think that you did not take into account well enough the comment raised by Referee #2 (who also asked for a major revision, but unfortunately was unable to review the paper again during the summer break) about the focus of the paper. Yes, you rewrote parts of the introduction, shifting the focus to the IWV analysis based on the two (recent) reanalyses (page 2, line 33 - page 3, line 10), but this shift of focus is not consistently kept throughout the analysis. For instance, in Section 3, you should then primarily discuss the differences in the means and variability between the IWVs from the reanalyses, and in regions where you find discrepancies between both reanalyses, use the GPS dataset to understand and explain those discrepancies. Here, also the reference to the analysis done by Trenberth et al. 2011 is important. Now, in its present form, two third of the Section (pages 7 and 8) deals with GPS - ERA-Interim IWV differences, while the focus was said to lie on the reanalyses. These two pages should hence almost completely be dropped from the regular text, instead I would devote an entire appendix on GPS site specific findings (with a description (and explanation) of sites for which the means, standard deviation and trends deviate from these of the reanalyses). In this case, a reader with a GPS background will easily find his/her way to relevant information for his/her research. The same remark about the inconsistent focus applies to the trend description sections 4 and 5.1. As your focus is on the comparison of the reanalyses, it is really illogical to start the description the trends with the comparison between GPS and ERA-Interim (Section 4). From my point of view, it seems more logical to start the analysis with the comparison of the ERA-Interim and MERRA-2 trends for the 1980-2016 time period, and then constrain to the 1995-2010 time period in which the GPS dataset can be used as external comparison (as outlined on page 3, lines 5-6). But here again, I would move GPS site specific findings about trend differences with ERA-Interim (and why not with MERRA-2) to the dedicated Appendix.

We thank the editor for the constructive comments that helped improve the manuscript. The paper was significantly shortened keeping in mind these comments, including a reorganization of the subsections. The focus was first put on a general intercomparison between GPS and reanalyses for the longest common period between the datasets (with more station-specific comparisons between ERA-Interim

and GPS moved to an Appendix, as suggested). And then followed by a more extensive comparison between the two reanalyses, in term of trends, for an extended period (largest common period between reanalyses). We believe this new organization of the paper, aside from making it shorter, will also make it easier to read.

Now, I will give some specific comments, in particular highlighting the parts of the paper that can seriously be shortened to my opinion.

- * page 1, lines 12-13: in the abstract you mention the link with ENSO, while this is only a secondary outcome of your paper (as a matter of fact, you have never shown it). So drop it.

The lines have been dropped from the manuscript.

- * page 2, lines 5-13: also not very relevant for your analysis here.

These lines have been removed

- * page 3, lines 1-4: move to section 2.1

This has been done.

- * page 4, lines 7-10: might be moved to the GPS site-specific appendix

They have been moved to Appendix 2, as suggested.

- * page 6: lines 14-19: Is this information (mentioned, not shown) really important for your paper?

The information has been removed.

- * page 6, lines 24-26: how does this finding compare with other studies (e.g. Trenberth et al. 2011? Perhaps you should mention this at this location).

The Trenberth et al. (2011) paper does not deal with MERRA-2 data, although it was used a reference throughout the paper.

- * page 7, lines 4-25: this information might be shifted to the proposed appendix

It has been moved to Appendix 2, as suggested.

- * page 7, line 31 - page 8, line 28: this information might be shifted to the proposed appendix, possibly just provide a summary of a few sentences in this part of your regular paper.

This has been done.

- * Sect 4: move after Section 5.1 and shift the bulk of the text (especially page 9, line 15 - page 10, line 15) to the proposed appendix.

- * page 11, lines 14-22: please be aware of some duplication of text with sections 5.1 and 5.2

- * Sect 5.1: I would start this section with the paragraph on page 13, lines 19-33 (but only for the long period), which is really well written, a really good summary without too much obsolete information.

- * page 12, line 15 - page 13, line 12: these paragraphs could be considerably be shortened! You just have to mention where the ERA-Interim and MERRA-2 trends are opposite and what the trends of the GPS sites in those regions are.

Regarding the points above, the paper has been reorganized in large part, so that the text has been reduced overall, with less repetition. In this new version we start by comparing the three datasets (GPS, ERA-Interim and MERRA-2) for the longest common period (1995-2010), and then extend the trend analysis to 1980-2016 for the ERA-Interim vs. MERRA-2 comparison. When comparing the

datasets, we focus on the differences found between reanalyses and attempt to compare it with GPS.

* page 16, line 32 - page 17, line 11: this paragraph is very hard to follow, as it is a mixture of IWV trends, T trends, IWV-T correlations, both for the short and long period and also for the seasons! Could you not highlight the most important findings instead of mentioning them all?

This has been re-written :

The trend in T anomalies also stops at around 2008 (Fig. 12a). Before that period, the temperature anomaly is increasing significantly, despite strong month-to-month variability. However, there is low/negative correlation between IWV and T anomalies when considering the monthly time series (Fig. 12a). In JJA, the trends are strong and go on after 2008 (Fig. 12c). The correlation of anomalies for JJA between both reanalyses is quite good, both for IWV (around $r = 0.67$ for the short period and $r = 0.63$ for the longer period) and T (around $r = 0.69$ for both periods), although their amplitudes and trends are quite different. MERRA-2 presents an overall moistening trend, while ERA-Interim shows a drying (Fig. 7g,h and 12c). Simultaneously, the temperature trends are both positive and significant, thus not explaining the IWV trends according to C-C

* page 18, lines 5-12: In the beginning of the summary, you state that your focus are the modern reanalyses (line 3). But, in the following lines, you give the results about the comparison between GPS and ERA-interim.

These have been re-written :

The means and variability in IWV in the reanalyses were inter-compared and compared to ground-based GPS data for the 1995-2010 period. ERA-Interim was shown to exhibit a slight moist bias in the extra-tropics ($\sim 0.5 \text{ kg m}^{-2}$) and a slight dry bias in the tropics in relation to both GPS and MERRA-2, which is consistent with other studies (Trenberth et al., 2011). Inter-annual variability in ERA-Interim is highly consistent with GPS, and in good agreement with MERRA-2. Differences were pointed out between GPS and reanalyses at only a few stations, mostly located in coastal regions and regions of complex topography, where representativeness errors put a limit to the comparison of gridded reanalysis data and point observations.

Anonymous Referee #1

General Comments

The revised manuscript is 46 pages long. The previous version was 43 pages long and I gave the recommendation to shorten the manuscript and focus on what is new. (I did ask for the Appendix added in the updated version, but it is 1.5 pages long, and could be made significantly shorter.)

The revised manuscript has now been significantly shortened.

I think this is still a drawback in Sections 4 and 5. There is no need to "walk through" different regions repeating in words what is already presented in the figures. I would prefer if the authors could focus on issues (in terms of trends or mean values) where there are significant disagreements, given the uncertainties of the means and the trends.

Following this suggestion, sections 4 and 5 have been merged and reduced, focusing on the significant similarities and disagreements between reanalyses, with GPS being used as an independent comparison.

Specific comments

page 25, Table 1: Does it make sense to divide the seasons into DJF and JJA when you calculate mean values using data from sites spread over both the northern and the southern hemisphere?

The statistics in Table 1 have now been separated by hemisphere.

Technical Corrections

The technical corrections have been applied.

page 1, line 12: 20% --> 20 %

page 3, lines 7 and 8:

page 7, lines 17 and 20: "space" between values and units is missing

page 17, line 12: 925hPa --> 925 hPa

page 18, line 9: 20% --> 20 %

page 46: Figure A3 --> Figure A1 ?

Anonymous Referee #3

The paper consists of an analysis of the trends and variability of integrated water vapor mainly in the period 1995-2010, mainly analyzing ERA-Interim product in comparison with reliable local data (GPS) and another reanalysis, MERRA-2. The manuscript is very well written, and very thorough both in all of its sections. Maybe it can feel dense because of its length, and a shortening could make it easier to read. The statistical treatment is very good to my knowledge. The topic is very interesting and of paramount importance.

I only have a few questions that I would like the authors to address:

1. Authors claim that the GPS time-series have inhomogeneities. I would like to know if they have considered any kind of statistical treatment to eliminate these inhomogeneities (when it is clear that they are due to GPS and not to ERA-Interim), to see if after correction they match ERA-interim trends.

Not yet. At this point the method of eliminating inhomogeneities uses ERA-Interim data, so that ERA-Interim could not be used as comparison. This is an ongoing reasearch topic.

2. Page 2, line 6: IPCC report is mentioned, but not the year, and it does not appear in references section.

The IPCC is no longer cited/ mentioned.

3. Page 2, lines 32-33: could the authors give references to these "several studies"?

Yes, a more thorough overview of the studies is now given (i.e. : Sherwood et al. (2010), Trenberth et al. (2005) among others)

4. Page 5, line 1: could the authors provide a references to NASA JPL's product?

Basic details on the operational GPS data processing procedure are described by Byun and Bar-Server (2009).

<http://igscb.jpl.nasa.gov/pipermail/igsmail/2010/007488.html>

5. Page 6, line 4: author claim that interoplation is done with the "4 surrounding grid points". Does this mean that they use the closest north, east, south, west grid points but not the grid point coincident with the GPS location?

GPS locations do not coincide with the reanalyses grid points, so we use the 4 gridpoints on the summit of the square enclosing the GPS station. This is a standard method for bi-linear interpolation.

6. Page 8, line 24-25: Since the test is not very efficient because of the low number of points, have authors considered using, for instance, monthly averages, in order to have more datapoints? Of course the time-series should be detrended first.

We didn't consider this option. It would give more data points but they would be noisier, so it is probable that their significance would not be higher.

7. Page 9, last line: Authors claim that "to be physically explained, such trends would imply a significant change in the regional and global water cycle". Could this be referenced, or explained?

The trend in ERA-Interim is -17% per decade, so -26% over the 15 years of the study. Such large trend has never been observed anywhere and is hard to explain.

8. I would suggest that Table S3 have significant trends in bold, or marked in any way to improve readability. But this is up to the authors to decide.

We provide the p-values so the reader can chose which confidence level he/she considers the most relevant.

9. Regarding lines 11-12 in page 15, I would like to know what other variables have been considered for "temperature proxy" and why T2m was chosen.

Actually, no other variables were tested, T2m was chosen from the beginning. In order to see the link between water vapour trends and surface temperature trends, especially in a context of climate change. This is following studies by, for instance, Trenberth et al. (2005) and Wang et al. (2016) that also looked at this relationship (cited in the paper).

10. Page 16, line 4: CMIP5 is firsts used here, so the meaning of the acronym should be provided. A reference here would be appropriate as well.

The acronym is now defined in the manuscript.

11. Figures 12 and 15: The figures show the trend spatially averaged. Could the authors explain how the computation of spatial averages was performed?

The IWV anomaly values were averaged over the box, and a trend of the resulting time series was computed.

12. Table S3: p-values do not need so many decimal places, these should be rounded to 3 decimal places.

This has been done in the new version of the supplement.

Global IWV trends and variability in atmospheric reanalyses and GPS observations

Ana C. Parracho^{1,2}, Olivier ~~Boek~~¹Bock², Sophie ~~Bastin~~²Bastin¹

¹IGN¹LATMOS/IPSL, Sorbonne Université, UVSQ, CNRS, Paris, France

²IGN LAREG, Université Paris Diderot, Sorbonne Paris Cité, Paris, 75013, France;

³LATMOS/IPSL, UVSQ, Université Paris-Saclay, Sorbonne Universités, UPMC, Univ., Paris 06, CNRS, Guyancourt, France

Correspondence to: Ana C. Parracho (ana-claudia.parracho@etu.upmelatmos.ipsl.fr)

Abstract.

This study investigates the means, variability, and trends in Integrated Water Vapour (IWV) from two modern reanalyses (ERA-Interim and MERRA-2) from 1980 to 2016 and ground-based GPS data from 1995 to 2010. It is found that the mean distributions and inter-annual variability in IWV in the reanalyses and GPS are consistent, even in regions of strong gradients. ~~Inter-annual variability is dominated by ENSO with variations as large as 20% IWV in the tropics and the mid-to-high northern latitudes in winter.~~ ERA-Interim is shown to exhibit a slight moist bias in the extra-tropics and a slight dry bias in the tropics (both ~~in on~~ the order of 0.5 to 1 kg m⁻²) compared to GPS. ERA-Interim is also generally drier than MERRA-2 over the ocean and within the tropics. Differences in variability and trends are pointed out at a few GPS sites, which ~~might beare~~ due to representativeness errors, for sites located in coastal regions and regions of complex topography, gaps and inhomogeneities ~~in the GPS series;~~ due to equipment changes in the GPS series, and potential inhomogeneities in the reanalyses, due to observing system changes. Trends in IWV and surface temperature in ERA-Interim and MERRA-2 are shown to be consistent, with positive IWV trends generally correlated with surface warming, but MERRA-2 presents a more general global moistening trend compared to ERA-Interim. Inconsistent trends are found between the two reanalyses over Antarctica and most of the southern hemisphere, and over central and northern Africa. The uncertainty in current reanalyses remains quite high in these regions where few in-situ observations are available and the spread between models is generally important. Interannual and decadal variations in IWV are also shown to be strongly linked with variations in the atmospheric circulation, especially in arid regions, such as North Africa and Western Australia, which add uncertainty in the trend estimates, especially over the shorter period. In these regions, the Clausius-Clapeyron scaling ratio is found not to be a good humidity proxy for interannual variability and decadal trends.

Mis en forme : Police :10 pt

Mis en forme : Non Exposant/ Indice

1 Introduction

Water vapour is a key component of the Earth's atmosphere and plays a key role in the planet's energy balance. It is the major greenhouse gas in the atmosphere and accounts for about 75 % of the total greenhouse effect globally (Kondratiev, 1972). The total amount of water vapour is mainly controlled by temperature, closely following the Clausius-Clapeyron (C-C) equation (Schneider et al., 2010). Water vapour is thus an important part of the response of the climate system to external forcing, constituting a positive feedback in global warming (Held and Soden, 2006). However, at a regional scale, deviations from C-C law are observed and the strength of the feedback can vary, also because the radiative effect of absorption by water vapour is sensitive to the fractional change in water vapour, not to the absolute change (O'Gorman and Muller, 2010).

~~The spatial structure of global IWV variability at seasonal and longer time scales evidences patterns that result from interactions between the atmospheric circulation and the land and ocean surfaces and are dominated by El Niño Southern Oscillation (ENSO) (Trenberth et al., 2005).~~

~~Although El Niño events are associated with increasing temperatures in the eastern and central Pacific with impact on the global weather and climate, it is not well known if global warming will lead to more frequent or intense El Niño events (Collins et al., 2010). Another strong cause of variability in the northern hemisphere is the North Atlantic Oscillation (NAO). A high positive NAO is associated with warmer winters in the Eurasian landmass, due to the stronger westerly and south westerly airflow that brings in warmer maritime air. However, it is not clear how the phase or intensity of NAO has been, or will be, affected by climate change (Visbeck et al., 2001).~~

~~All these parameters, This~~ and the fact that the ~~time of residence time~~ of water vapour in the atmosphere is short, make IWV a highly variable component and its study in terms of variability and trends is rather challenging. Sherwood et al., (2010) compared the long-term IWV trends reported in several studies using different datasets. Although there appears to be a global positive trend in the overall IWV data, which is consistent with a global warming trend, it is difficult to compare results from different studies, as they refer to different data sources, time periods and different sites and spatial coverage. Trenberth et al. (2005) found major problems in the means, variability, and trends from 1988 to 2001 for the National Centers for Environmental Prediction (NCEP) reanalyses 1 and 2, and for the 40-year European Centre for Medium-Range Weather Forecasts (ECMWF) reanalysis (ERA-40) over the oceans. The reanalyses showed reasonable results over land where they are constrained by radiosonde observations. Only the reprocessed IWV data from the special sensor microwave imager (SSM/I) appeared to be realistic in terms of means, variability, and trends over the oceans. Their work points to two important issues. First, the reanalyses generally lack assimilation of water vapour information and suffer from model biases and, in the case of ERA40, problems in bias corrections with new satellites (namely after major volcano eruptions). Second, they highlight the need for the reprocessing of data, and point to the shortcomings in reanalyses due to the changing observing system. The bias correction of new satellite radiances in the ECMWF reanalysis system has recently been improved using a variational bias-correction scheme, including the detection of instrument calibration errors and long term drifts, as well as volcano eruptions (Dee and Uppala, 2009). Reduction of model biases and enhanced assimilation capabilities of satellite data (e.g. rain-affected

Mis en forme : Retrait : Première ligne : 0,5 cm

radiances) have generally improved the water cycle in modern reanalyses. Reanalyses data ~~agree thus~~ generally agree well at representing the short-term variability (e.g. El Niño-Southern Oscillation, ENSO) but their ability for detecting climate trends is still debated (Dessler and Davis, 2010; Thorne and Vose, 2010; Trenberth et al., 2011; Robertson et al., 2014; Schröder et al., 2016). Chen and Liu (2016) compared the global variability and trend in water vapour in ERA-Interim and NCEP with GPS, radiosonde and microwave satellite data, and found that ERA-Interim had better accuracy than NCEP.

In this study we will focus on analysing the mean distributions, inter-annual variability, and decadal trends from two recent reanalyses, ECMWF reanalysis ERA-Interim (Dee et al., 2011), referred to as ERAI, and the 2nd Modern-Era Retrospective analysis for Research and Applications, MERRA-2 (Gelaro et al., 2017). ~~MERRA-2The IWV contents from benefits from recent developments in NASA's Goddard Earth Observing System (GEOS) model suite intended to address the impact of the changes in observing system (Gelaro et al., 2017). As a result, atmospheric water balance and variability in MERRA-2 are more realistic, though variations of IWV with temperature are weaker in the main satellite data reanalyses (namely ERA-Interim and MERRA-2) compared to microwave satellite observations over the oceans (Bosilovich et al., 2017). Here, the IWV contents of~~ the two reanalyses are intercompared and compared to a global, homogeneously reprocessed Global Positioning System (GPS) dataset over ocean and land. The ground-based GPS observations are independent from the reanalyses as they are ~~so far~~ not assimilated and constitute thus a valuable validation data ~~for atmospheric reanalyses (Bock et al., 2007) and satellite data (Mears et al., 2015).~~ A critical assessment of the homogeneity of GPS dataset itself ~~is provided throughout the~~ was made during this study as previous work detected small offsets associated to GPS equipment changes (Vey et al., 2009; Ning et al., 2016).

Furthermore, to add new insights in both the evaluation of ERA-~~interim~~Interim and MERRA-2 reanalyses and in the understanding of IWV trends and variability, we separate the analysis into seasons, and consider trends and interannual variability of seasons. This analysis by seasons is rarely provided in other studies, although it helps to better identify regions with higher uncertainty and to understand the physical processes involved in different seasons (e.g. the dynamical component which transports moisture strongly differs between winter and summer). Trenberth et al. (2011) separated January and July in their analysis of the representation of water and energy budget in ERA-~~Interim~~ and MERRA and showed the importance ~~to study of studying~~ the seasons separately. Compared to this study, we added the analysis of the GPS dataset and use ~~the new version of~~MERRA-2 which benefits from several updates compared to MERRA.

This paper is organized as follows. Section 2 details the datasets and methods ~~used~~. Section 3 reports on the means and variability found in the GPS and reanalyses data; for the 1995-2010 period. Section 4 ~~focuses on the monthly and seasonal analyses~~ trends in GPS and from ERA-Interim, for 1995-2010. In Section 5 we confront results of ERA-Interim and GPS to and MERRA-2. In this section, the comparison between ERA-Interim and MERRA-2 was also extended to the over the longer 1980-2016 period and focused on two regions of intense trends: western Australia and north Africa/eastern Sahel. Section 6 summarizes and concludes the paper.

Mis en forme : Non Exposant/ Indice

Mis en forme : Police par défaut

2 Datasets and methods

2.1 Reanalysis data

In this study we use two modern reanalyses: the ECMWF reanalysis, ERA-Interim (Dee et al., 2011), and the NASA reanalysis, MERRA-2 (Gelaro et al., 2017). ERA-Interim is the successor of ERA-40 and benefits from many improvements, especially a variational bias-correction scheme which reduces the impact of observing system changes. It is thus expected that trend estimates are more realistic. MERRA-2 is an update of MERRA which benefits from recent developments in NASA's Goddard Earth Observing System (GEOS) model suite intended to address the impact of the changes in observing system (Gelaro et al., 2017). As a result, atmospheric water balance and variability in MERRA-2 are more realistic, though variations of IWV with temperature are weaker in the main satellite data reanalyses (namely ERA-Interim and MERRA-2) compared to microwave satellite observations over the oceans (Bosilovich et al., 2017). Reanalysis data from the ECMWF, ERA-Interim (Dee et al., 2011), and NASA, MERRA-2 (Gelaro et al., 2017), were extracted for the

Data from both reanalyses were extracted for the common 1980-2016 period, on regular latitude-longitude grids, at their highest horizontal resolution (0.75° x 0.75° for ERA-Interim and 0.625° longitude x 0.5° latitude for MERRA-2). In this work, the two-dimensional (2D) distribution of IWV is investigated with reanalysis fields and with point observations from 404 GPS data. Because GPS antenna heights and surface heights in the reanalyses are not perfectly matched (see the GPS coordinates and the heights for both reanalyses in the supplement Table S1), the IWV estimates were adjusted for the height difference Δh based on an empirical formulation derived by Bock et al., 2005: $\Delta IWV = -4 \cdot 10^{-4} \cdot IWV \cdot \Delta h$, with Δh in m. The advantage of this formulation is that it can be applied directly to the IWV data without requiring any auxiliary data. Its accuracy was checked compared to a more elaborate formulation using ERAI pressure level data (see Appendix B). The corrections were thus computed for each reanalysis separately using the monthly IWV data from the nearest grid point to every GPS station.

2.2 GPS data

We used the reprocessed tropospheric delay data from GPS stations of the International GNSS (Global Navigation Satellite System) Service (IGS) network (Fig. 1). Because GPS heights and surface heights in the reanalyses are not perfectly matched (see the GPS coordinates and ERA-Interim heights in the supplement Table S1), the IWV estimates were adjusted for the height differences using two different methods. In the 2D maps (e.g. Fig. 2), the monthly mean GPS IWV estimates were height corrected to match the nearest reanalysis grid point, while for the computation of IWV differences (e.g. Fig. 4), a more elaborate interpolation method was used (described below). For the monthly mean IWV correction, specific humidity from the ERA-Interim pressure level data were integrated over the layer of atmosphere bounded by the model's surface height and the height of the GPS station. The ERA-Interim pressure level data contain a total of 37 levels between 1000 and 1 hPa, among which 27 levels lie between 1000 and 100 hPa. This ensures a good vertical sampling of the troposphere where most of the

Mis en forme : Titre 1

water vapour is located. Note that for the sake of consistency, the same pressure-level data (i.e. ERA-Interim) are used for correcting the MERRA-2 monthly mean IWV data shown in the maps.

In the case of ERA-Interim, the height differences between GPS stations and nearest model grid points range from -1457 m (at the SANT (Santiago, Chile) station) to +3167 m (at the MKEA (Mauna Kea, Hawaii) station). The negative height difference means GPS height is below the model surface. The mean IWV corrections for these two stations amount to -3.4 kg.m⁻² and 21.7 kg.m⁻², respectively. Globally, inter-quartile range of the corrections is [-1.40, 0.39] kg.m⁻².

A more rigorous approach is adopted for the quantitative evaluation of the reanalysis IWV data with respect to GPS IWV data, in order to minimize temporal and spatial sampling issues. In this case, we time-matched the 6-hourly data and performed a spatial interpolation of the reanalysis IWV estimates to the latitude and longitude of the GPS site. A bilinear spatial interpolation is computed from the model IWV estimates at the 4 grid points surrounding each GPS station. The IWV model estimates are then recomputed from the pressure level data by vertically integrating the specific humidity between the height of the GPS station and the top of the atmosphere. Most GPS station heights fall between two pressure levels and the specific humidity data can be interpolated. However, for stations located below 1000 hPa (the lowest pressure level) the reanalysis data are extrapolated. Interpolation and extrapolation are done linearly for specific humidity and temperature, and exponentially for pressure. This procedure minimizes differences between the reanalysis IWV data and the GPS estimates with better results than previous correction methods (e.g. Bock et al., 2014). However, a perfect match between observations and model data is hindered by representativeness errors (Lorenc, 1986), especially in mountainous and coastal regions.

2.2 GPS data

The ~~was~~ reprocessed GPS data set used in this work was produced by the NASA Jet Propulsion Laboratory (JPL) in 2010-2011, and is referred to as IGS repro1. Basic details on the operational GPS data processing procedure are described by Byun and Bar-Server (2009). ~~Compared to~~ for the operational version at the time, the The reprocessed data set was produced with more recent observation models (e.g. mapping functions, absolute antenna models) and consistently reprocessed satellite orbits and clocks (IGSMail-6298). Inspection of file headers revealed that the processing options were not updated for a small number of stations for a period of nearly one year between March 2008 and March 2009. The comparison of solutions with old and new processing options (available for year 2007) showed that this inconsistency in the processing has negligible impact at most stations, except for stations at high southern latitudes (e.g. in Antarctica). The data set covers the period from January 1995 to December 2010 for 456 stations. Among these, 120 stations have time series with only small gaps over the 15-year period. However, the geographical distribution is quite unequal between hemispheres and even within a given hemisphere, with namely a cluster of 20 stations in the western USA with inter-station distance smaller than 0.75°. In order to avoid over-representation of this region, 16 out of these 20 stations have been discarded (the selection retained those with the longer time series). The final GPS IWV dataset used in this study is thus limited to the selected 104 stations.

The basic GPS tropospheric observables in this study are the Zenith Tropospheric Delay (ZTD) estimates which are available at a 5-minute temporal resolution, min sampling in the IGS repro1 dataset. The GPS ZTD data were screened using

Mis en forme : Retrait : Première ligne : 0,5 cm

an adaptation of the methods described by Bock et al. (2014) and Bock et al. (2016). First, we applied a range check on the ZTD and formal error values using fixed thresholds ~~representing according to~~ the spatial and temporal range of expected values: 1 – 3 m for ZTD and 0 – 6 mm for formal errors. Second, we applied an outlier check based on site-specific thresholds. For ZTD, values outside the median ± 0.5 m ~~are were~~ rejected and, for formal errors, values larger than 2.5 times the median ~~are were~~ rejected. The ~~median ZTD and formal error values are updated yearly~~ thresholds were recomputed for every year. Using these thresholds, we detected no ZTD values outside the limits. This is because the limits were sufficiently large to accommodate for the natural variability of ZTD values (Bock et al., 2014). On the other hand, the formal error check rejected ~~8.8x108~~ 10^{-4} (i.e. less than 0.1 %) of the data overall. After screening, the 5-~~minutemin~~ GPS ZTD data were averaged in 1-hourly bins.

The conversion of GPS ZTD to IWV was done using the following formula: $IWV = ZWD \times \kappa(T_m)$. Where $\kappa(T_m)$ is a function of weighted mean temperature T_m , and ZWD is the zenith wet delay, obtained from: $ZWD = ZTD - ZHD$ and ZHD is the hydrostatic zenith delay (see Wang et al. (2005) or Bock et al. (2007) for further details). In this work, the surface pressure used to compute ZHD and the temperature and humidity profiles necessary to obtain T_m were obtained from ERA-Interim pressure level data. The profile variables are first interpolated or extrapolated to the height of the GPS stations at the 4 surrounding grid points and then interpolated bi-linearly to the latitude and longitude of the GPS stations. At this stage, the 1-hourly ZTD GPS data and the 6-hourly ERA-Interim data (ZHD, T_m , and IWV) were time-matched (within ± 1 hour) ~~for both the ZTD to IWV conversion and IWV intercomparison.~~

Afterwards, monthly means of the 6-hourly IWV estimates are computed and those months which have less than 60 values (i.e. at least half of the expected monthly values) are rejected. Seasonal means are computed from the monthly values when at least 2 out of 3 months are available. These selection criteria ensure that the computed values are representative of the monthly and seasonal means.

In this work, inhomogeneities in the GPS IWV time series due to equipment changes were not corrected a priori, as the existing metadata may not be complete, but were rather detected and discussed during the course of the intercomparison with ERA-Interim. ~~This work is a preliminary contribution to a more extensive detection (see Appendix B). Detection and correction effort of inhomogeneities in the GPS ZTD and IWV data is a subject of on-going research.~~

2.3 Computation of trends

The linear trends were computed using the Theil-Sen method (Theil, 1950 and Sen, 1968), a non-parametric statistic that computes the median slope of all pairwise combinations of points. This method is described in more detail in the Appendix A to this paper, where it is also compared with another commonly-used method for trend estimation, the Least Squares method.

The Theil-Sen method was applied to the anomalies obtained by removing the monthly climatology from the monthly data. In the case of seasonal trends, the mean anomalies for the months of December, January and February (DJF); and June, July and August (JJA) were used ~~(when there are at least two months of data available per season, per year).~~. The statistical significance

Mis en forme : Police :Non Italique

Mis en forme : Police :Non Italique

Mis en forme : Retrait : Première ligne : 0,5 cm

Mis en forme : Titre 2

of the monthly and seasonal trends was assessed using a modified Mann-Kendall trend test (Hamed and Rao, 1998), which is suitable for autocorrelated data, at a 10 % significance level.

3 Means and variability in 3 Comparison between GPS and reanalyses IWV (1995-2010)

3.1 Means and variability in IWV

5 The reanalyses and GPS data have been used to investigate the mean seasonal IWV distribution and ~~its~~their interannual variability for ~~December-January-February (DJF) and June-July-August (JJA).~~

are presented in Fig. 2. In the maps of the means (Figs. 2a, b), we can see that ERA-Interim reproduces the spatial variability well compared to GPS, including the sharper gradients in IWV, for instance, on the northern and southern flanks of the Intertropical Convergence Zone (ITCZ) in both seasons, and in the regions of steep orography (for example, along the Andes region, in South America).

10 For the analysis of the interannual variability we computed the relative standard deviation of the seasonal IWV time-series (i.e. standard deviation of seasonal time series divided by its mean value). The relative variability emphasizes both regions where the variability is high compared to the mean IWV (e.g. the tropics) and ~~regions where the mean IWV contents are small (e.g. cold-dry polar and/or mountainous regions and warm-dry desert areas).~~ In DJF (Fig. 2c), strong interannual variability (> 15 %) is found for northern high-latitude regions (north-eastern Canada and eastern Greenland, polar-Arctic area, and a large part of Russia and north-eastern Asia) and for the tropical arid regions (Sahara, Arabic peninsula, central Australia). Some correlation is found between the seasonal IWV anomalies and the North Atlantic Oscillation (NAO) index (Barnston and Livezey, 1987) (not shown) over Siberia ($r = 0.5$) and Greenland ($r = -0.5$). Noticeable variability is also seen in the central tropical Pacific in DJF but this is due to the extremely large variability in absolute IWV contents (up to $6 \text{ kg} \cdot \text{m}^{-3}$) associated with the ENSO. Linear correlation coefficients between the seasonal IWV anomalies and the Multivariate ENSO Index (MEI; Wolter and Timlin, 1993, 1998) in this region reach $r = 0.80$ (not shown). In JJA, large interannual variability is observed mainly over Antarctica and Australia (Fig. 2d). ~~Locally enhanced variability is also seen over the Andes cordillera, but this is mainly due to the very low IWV values at high altitudes.~~

20 Similar mean patterns are observed in MERRA-2 for both seasons, although maximum values over the ITCZ have different intensities: ~~(not shown)~~. In order to better gauge the differences, mean difference fields between MERRA-2 and ERA-Interim are shown (Figs. 3a and b). It is observed that ERA-Interim is generally drier than MERRA-2 over the ocean and in the regions of maximum IWV, and moister in the southern part of South America, north and south of the ITCZ over Africa, and in southern ~~(DJF) and central (JJA) Asia~~ central Asia in DJF (JJA). This result is consistent with differences between ERA-Interim and MERRA reported by Trenberth et al. (2011).

30 ~~In terms~~Comparing the reanalyses with GPS in Fig. 4 a-d shows that both reanalyses are too moist in the northern hemisphere in both seasons, ERA-Interim has a dry bias at the tropical sites, more pronounced in DJF, while MERRA-2 has a moist bias overall but more pronounced in the southern hemisphere in DJF, especially over Australia, and in the northern

Mis en forme : Titre 1

hemisphere in JJA (see the increased bias over North America, northern Europe and Asia). Hemispheric and seasonal statistics can be found in Table 1 which show namely that in the northern hemisphere, the median biases of the reanalyses are very consistent in DJF (0.5-0.6 kg.m-2) while in JJA the bias in MERRA-2 (1.1 kg.m-2) is nearly the double of the bias in ERA-Interim (0.59 kg.m-2). In the southern hemisphere the main difference is for the DJF bias which is nearly null in ERA-Interim and 0.7 kg.m-2 in MERRA-2. Similar conclusions can be drawn from the relative biases. High consistency is also seen in dispersion of the biases (inter-quartile range) between both reanalyses, with larger absolute values in the summer hemisphere and larger relative values in the winter hemisphere.

Note that in Fig. 4a-d GPS estimates at a number of sites show large biases with respect to both reanalyses. These sites are generally located in coastal regions and/or regions with complex topography where representativeness differences can be suspected (Lorenc, 1986). We applied a statistical test to detect stations with significant differences in the mean values (with 99% confidence level). When GPS and ERA-Interim are compared, 20 stations are detected in DJF and 17 in JJA, while with MERRA-2, 26 stations are detected in DJF and 44 in JJA. These numbers confirm in a more objective way the visual interpretation of Fig. 4. The values of all statistics can be found in Supplement Table S2.

For the analysis of the interannual variability, for DJF, there are similar maxima of we computed the relative standard deviation of the seasonal IWV time series (i.e. standard deviation of seasonal time series divided by its mean value). The relative variability emphasizes regions where the mean IWV contents are small (e.g. cold dry polar and/or mountainous regions and warm dry desert areas). In DJF (Fig. in ERA-Interim and MERRA-2 over the Arctic, Tropical Pacific, and Siberia and West Africa (to a lesser extent). Over Australia2c), strong interannual variability (> 15 %) is found in ERA-Interim for northern high-latitude regions (north-eastern Canada and eastern Greenland, polar Arctic area, and a large part of Russia and north-eastern Asia) and for the tropical arid regions (Sahara, Arabic peninsula, central Australia). There are similar patterns of variability in MERRA-2 (not shown), with slightly higher variability in MERRA-2 over India and Antarctica; the variability is lower in MERRA-2 than in ERA-Interim, while over Canada the variability is higher. The difference fields between MERRA-2 and ERA-Interim highlight these differences (Fig. 3c). Although some of the areas of interest are not covered by the long-term GPS observations, in general, there is better agreement between GPS and ERA-Interim than MERRA-2, especially at higher latitudes. For JJA (Fig. 3d), the intense variability in Australia and the Andes seen in ERA-Interim (and GPS) is not as intense in MERRA-2, while a stronger In JJA, large interannual variability is observed in ERA-Interim mainly over Antarctica and Australia (Fig. 2d). Locally enhanced variability is also seen over the Andes cordillera, but this is mainly due to the very low IWV values at high altitudes, for MERRA-2 over Antarctica. MERRA-2 has similar patterns of IWV variability, with lower variability over North Africa and north of the Andes, and higher variability over Antarctica (Fig. 3d). The mean IWV differences are shown in Figs. 4a and b for all 104 GPS sites. It can be noticed that the negative differences (ERA-Interim IWV lower than GPS IWV) are almost all within the ITCZ, with few exceptions in north-western North America and in Antarctica. This result is confirmed when ERA-Interim is compared to MERRA-2 and consistent with differences between ERA-Interim and MERRA-2 reported by Trenberth et al. 2011. A paired two-sample t-test detected 20 stations with significant differences in the mean IWV values at 0.01 confidence level in DJF and 17 in JJA (the values for all stations can

Mis en forme : Retrait : Première ligne : 0,5 cm

be found in Supplement Table S2). The sites with most notable differences, either absolute (in $\text{kg}\cdot\text{m}^{-2}$) or relative (in %) are: CFAG in the Andes cordillera with a bias of $6.5\text{ kg}\cdot\text{m}^{-2}$ (26 %) in DJF and $3.9\text{ kg}\cdot\text{m}^{-2}$ (43 %) in JJA and, SANT in Chile with $-2.4\text{ kg}\cdot\text{m}^{-2}$ (15 %) in DJF, and TSKB (in Japan) with $1.9\text{ kg}\cdot\text{m}^{-2}$ (24 %) in DJF. In JJA, four other sites have large biases: KIT3 in Uzbekistan with a value of $6.2\text{ kg}\cdot\text{m}^{-2}$ (35 %), POL2 in Kirghizstan with $3.1\text{ kg}\cdot\text{m}^{-2}$ (20 %), SYOG in Antarctica with $0.6\text{ kg}\cdot\text{m}^{-2}$ (32 %), and MAW1 in Antarctica with $0.4\text{ kg}\cdot\text{m}^{-2}$ (31 %). The inspection of the time series shows that at some of these stations the biases are not constant in time but contain large seasonal variations, such as e.g. at CFAG (Fig. 5a) or KIT3 (Fig. 5b). These sites are located in coastal regions and/or regions with complex topography. Although we used an elaborate spatial and temporal matching of reanalysis and GPS data, representativeness errors are suspected to be the cause of these biases. To investigate this point, we compared the (vertically adjusted) IWV values from the 4 grid points surrounding each GPS station to the interpolated IWV values (see Section 2). We found that at CFAG, KIT3, POL2, SYOG, and MAW1, the interpolated values did not minimize the IWV biases between the reanalysis and GPS. This is explained by large variations in the altitude of the grid points at these sites (between 500m and 1000m) and the difficulty for the vertical interpolation method to properly predict the IWV variations over such large altitude ranges. In the case of SANT, although the interpolated value matches the GPS value better than any of the four surrounding grid point values, there is still a large bias explained by a variation in the altitude of the grid points of over 1500m. Statistics computed over all stations are given in Table 1. They indicate that ERA Interim is slightly moister on average than GPS. The median bias is $0.51\text{ kg}\cdot\text{m}^{-2}$ (6.2 %) in DJF and $0.52\text{ kg}\cdot\text{m}^{-2}$ (2.7 %) in JJA, and the standard deviation of the bias across the network amounts to $0.83\text{ kg}\cdot\text{m}^{-2}$ (6.9 %) in DJF and $0.95\text{ kg}\cdot\text{m}^{-2}$ (7.8 %) in JJA. As noticed above, there is some spatial variation in the mean difference, namely a negative mean difference in the tropics (ERA Interim < GPS) which is compensated in the global median by the larger number of stations in the extra-tropics which have a positive difference (ERA Interim > GPS).

Most of the marked regional features of interannual variability are also confirmed by GPS observations (Figs. 2e, d). One can especially notice the good representation of the relative variability over Australia or South America, both in DJF and JJA, and in the northern high latitudes, where the gradients are strong and well captured. However, a few stations show different values compared to the ERA Interim background. Figures 4c and d show the differences of relative standard deviations. The overall statistics are given in the second part of Table 1. They indicate a median difference close to zero for both DJF and JJA with a standard deviation across the stations of 1.7 % in DJF and 4.1 % in JJA. We used a two sample F test to detect the stations where the variances differ significantly. However, this test detected only one result with a p-value < 0.01 (station MCM4 in JJA) and two with a p-value < 0.10 (MCM4 and CFAG in JJA). This statistical test is probably not very efficient in the case of our short time series (≤ 16 points). In JJA, the four stations with the largest differences (ERA Interim — GPS) are located in Antarctica: MCM4, SYOG, MAW1, and DAV1 with differences of -39 % (p=0), -7.7 % (p=0.63), -4.8 % (p=0.81), and +3.9 % (p=0.27), respectively. In DJF, the largest differences are found for MKEA (Hawaii) and SYOG, where they amount to -11.4 % (p=0.52) and -4.8 % (p=0.30), respectively. Table S2 in the supplement provides the results for all stations. In the case of SYOG, MAW1, and DAV1, representativeness errors are suspected again because of the large variability in the IWV values of the surrounding grid points connected with large variations in the altitudes ($\geq 500\text{m}$) of these grid points. In the case of

MKEA, the variation in the altitude of the surrounding grid points is quite small because of the limited imprint of Mauna Kea Island on the 0.75° resolution grid of ERA-Interim. However, the difference in altitude between the GPS station and all four grid points is larger than 3000 m which is far beyond the prediction capability of the interpolation method described in Section 2. In the case of MCM4 and SYOG, the inspection of the time series of monthly mean IWV and IWV differences (shown in Figs. 5c and d) reveals variations in the means which coincide with GPS equipment changes and processing changes and unexplained variations in the amplitude of the seasonal cycle resulting in a marked oscillation in the monthly mean differences (ERA-Interim - GPS). Variations in the means introduce a spurious component of variability in the GPS IWV series (e.g. In general, most of the marked regional features of interannual variability are confirmed by GPS observations (Figs. 2c, d) at MCM4 the standard deviation of GPS IWV is 0.78 kg m⁻² compared to 0.21 kg m⁻² for ERA-Interim).

Three possible causes for the differences in the IWV means and variability between GPS and ERA-Interim exist. As already discussed above, representativeness differences are expected in regions of complex terrain where the environmental conditions can differ. Strong horizontal gradients in IWV are a limitation for the bi-linear horizontal interpolation that we used. This kind of situation is generally encountered when the altitudes of the grid points surrounding the stations are very different (e.g. AREQ, SANT, KIT3, MAW1, SYOG, POL2). This problem is enhanced when the altitude of the GPS station is below the model surface (e.g. SANT, AREQ, KIT3, MAW1, SYOG), because the model profile data are extrapolated below the ground, and/or the model and GPS surface altitudes are very different (e.g. MKEA). Representativeness errors due to large spatial variations in IWV and altitude are expected at 20 stations among which are those cited just above. However, they don't explain all the significant biases and differences in variability actually observed. The second aspect is connected with errors in the GPS data, e.g. However, a few stations show different values compared to the reanalyses, but their values don't impact the variability statistics shown in Table 1 thanks to the choice of median and inter-quartile range instead of mean and standard deviation. Based on the median values, Table 1 shows that in general ERA-Interim is in better agreement with GPS than MERRA-2, except for the Northern Hemisphere in JJA. It also shows that ERA-Interim has lower variability than GPS in the Northern hemisphere in both seasons (negative median value in Table 1), and higher variability in the southern hemisphere in JJA; while MERRA-2 has a lower variability throughout. Fig. 4 e-h show the spatial distribution of the differences for both reanalyses and seasons. Again, there is quite a large spatial dispersion (also revealed by the inter-quartile range in Table 1) with a number of outlying sites discussed in Appendix B.

Representativeness errors due to large spatial variations in IWV and complex topography are suspected at 20 stations. They contribute likely both to differences in the mean IWV values and in the variability. Errors in the GPS data, e.g. due to instrumental malfunctioning or measurement interferences, or changes in equipment resulting in variations in the mean IWV estimates are also suspected at a small number of sites. Such problems can be detected further confirmed by comparison with IWV measurements from nearby GPS receivers or from other collocated instruments such as DORIS or VLBI (Bock et al., 2014; Ning et al., 2016). The third cause stems from Lastly, errors in the reanalysis IWV data which reanalyses are expected suspected in data-sparse regions and regions where the performance of model physics and dynamics are poor. These can be diagnosed by comparing several reanalyses based on different models and different observational data or hypothesized

Mis en forme : Retrait : Première ligne : 0,5 cm

by eliminating the other causes. They are more difficult to diagnose. The differences observed between ERA-Interim and MERRA-2 might be due to a mix of differences in model physics and data assimilation.

43.2 Trends in GPS and ERA-Interim IWV (1995-2010)

Trends from ERA-Interim and MERRA-2 based on the time series of monthly means data (hereafter, referred to as monthly trends) are shown in Fig. 6. Significant-5. In general, there is continuity between oceanic and continental trends, suggesting a trend in air mass advections.

Both reanalyses show overall positive trends (moistening) are observed especially marked (statistically significant) in the tropics along the ITCZ, both over most of the tropical oceans and continents (northern South America, central Africa, and Indonesia in ERA-Interim), and at middle and high latitudes in the northern hemisphere. The moistening trends over the Arctic are significant in both reanalyses. They are interleaved with extended regions of negative (drying) trends are observed in which are statistically significant in both reanalyses over Australia, north/central Africa, over the south-tropical eastern Pacific region, west and on the oceanic border of the United States and generally south of 60°S. The Antarctic. The moistening/drying dipole structure in the south-eastern tropical Pacific area is consistent with the results of eastern equatorial Pacific has been observed by several authors using various satellite data and reanalyses over different periods (Trenberth et al. 2005; Mieruch et al., 2014) and is: Schröder et al., 2016; Wang et al., 2016). Trenberth et al. (2005) explained it as being due to the influence of different ENSO phases for this time period, as explained by Trenberth et al. (2005). Over land, significant positive trends are observed in the equatorial region along the ITCZ, especially in northern South America, Central Africa, and Indonesia, and in the northern hemisphere, especially over northern over the trends. The monthly trends computed at the GPS stations are consistent in sign and magnitude with the reanalyses where the reanalyses agree, except at a small number of GPS sites discussed in Appendix B. The trend values for ERA-Interim, MERRA-2 and GPS at all stations can be found in Supplement Table S3.

Significant differences between MERRA-2 and ERA-Interim are seen over several parts of the globe, in particular over the Maritime Continent, north/central Africa, central Asia, and Antarctica. In these regions the reanalyses show opposite trends. Such a discrepancy can be due to different representations of large scale moisture transport, surface-atmosphere processes, and data assimilation in the two reanalyses.

Over the Maritime Continent, ERA-Interim trends are positive while MERRA-2 trends are negative over the period from 1995 to 2010. Trenberth et al (2005) also reported strong moistening and warming trends over the region for the 1988-2003 period using SSM/I IWV data and NOAA SST data. Wang et al., 2016, confirmed the moistening but found a near-zero/slightly negative temperature trend for the 1995-2011 period (they used more recent releases of the SSM/I and NOAA data). Schröder et al. (2016) also found moistening trends in all their datasets over the 1988-2008 period, including SSM/I data and the MERRA reanalysis. Although not all studies concern the same period, they confirm the ERA-Interim results. This conclusion points to an inconsistent drying trend in MERRA-2 over the Maritime Continent. Comparison to the GPS IWV trends in Fig. 5a confirms

that ERA-Interim is in better agreement with the observations than MERRA-2, though the comparison is quite difficult because there are not many GPS stations available within the domain.

Over North America, Greenland, most of Europe and Siberia. Significant negative trends over land are observed over North Africa, Australia, Antarctica, central Asia, south of South America, and most of the USA. In general, there is continuity between oceanic and continental trends (e.g. North and South America, Central Africa), suggesting a trend in air mass advections. However, the magnitudes over Africa, the drying trend in ERA-Interim reaches an extremely large value of the larger trends (e.g. -3.5 kg m^{-2} per decade or -17% per decade over northern Africa) are) which is questionable. To be physically explained such trends, such a large trend would imply a significant change in the regional and global water cycle. Alternatively, they might be due to inhomogeneities in the observations assimilated in the reanalysis system. Comparison to GPS, that can hardly be supported by physical arguments. Unfortunately, there are no long-term GPS data available in the region. The trends in MERRA-2 over the region are smaller and more realistic, but they also show a different spatial pattern which is questionable as well. The drying in MERRA-2 extends southward over equatorial Africa, a region where moistening is expected to follow the observed warming trends (see Fig. 8). The difference between the reanalyses is further emphasized when comparing seasonal trends below. A major uncertainty in both reanalyses over this region is certainly due to the paucity in observations; when they are available, helps to address this question going into the assimilation. This statement is consistent with the results of Bauer (2009) and Karbou et al. (2010) who report a strong impact of humidity data from modern satellite instruments on the analysed moisture fields over the Sahara.

In general, the monthly trends computed at the GPS stations are consistent in sign and magnitude with ERA-Interim (Fig. 6). Many stations are operated in Europe and North America. Most of them show fairly consistent trends with ERA-Interim even in areas of marked gradients (e.g. between western Canada and the USA, or from central to western Europe). Australia is also well sampled with several stations, in the centre and along the coasts, and both the sign and spatial variations of trends are consistent (e.g. the eastern Australia's moistening trend). Many isolated stations in other regions confirm the ERA-Interim trends. Moistening trends are observed by stations (indicated in Fig.1) KOUR and BRAZ (northern part of South America); HRAO (South Africa), HISC (India), KELY (Greenland), DGAR (in the centre of the Indian ocean), FALE (in the Pacific Ocean), CRO1 (Puerto Rico), MAS1 (Canary Islands) and REYK (Iceland). In terms of drying trends, ERA-Interim and GPS trends are largely in agreement over the west coast of the United States, the southern half of South America (including the Andes region, which has steep IWV gradients) and the western half of Australia. It is also noteworthy that BRMU (in Bermuda) has a drying trend that is also captured in the ERA-Interim data. The results for all stations are given in the Supplement Table S3.

Inspection of Fig. 6 shows that there are a number of GPS stations where the trend estimates are large and of opposite sign compared to ERA-Interim: CCJM (south of the Japanese home islands), DARW (northern Australia), WUHN (eastern China), IRKT (central Russia), ANKR (Turkey), KOKB and MKEA (Hawaii), and MCM4 (Antarctica). Some of them (DARW, ANKR, KOKB, MKEA) are located in areas where the ERA-Interim trends change sign and a perfect spatial coincidence between the reanalysis and observations might not be expected. On the other hand, stations CCJM, WUHN, IRKT, and MCM4

Mis en forme : Retrait : Première ligne : 0,5 cm

are located within regions where the ERA-Interim trends are strong and significant, and extend over large areas. For some of these stations, the discrepancy is due to gaps and/or inhomogeneities in the GPS time series which corrupt the trend estimates. To mitigate the impact of gaps, time-matched series are also compared (Figs. 7a and b show the trend differences). The agreement is improved at DARW, ANKR and IRKT, and at many other sites (e.g. KELY in Greenland, SANT, MAW1).

However, there are still many sites with large differences. Table 2 lists the stations with the largest differences. Inspection of time series reveals the presence of large inhomogeneities at CCJM, MCM4 (already discussed in the previous section, see Fig. 5c, WUHN, SHAO, and CRO1. At CCJM (see Fig. 7a), the GPS minus ERA-Interim IWV difference time series has a large offset in 2001 which coincides with a GPS equipment change (receiver and antenna). This offset is responsible for a large negative trend estimate in the GPS series (-1.40 kg m^{-3} per decade) whereas the time-matched ERA-Interim series gives a positive trend ($+0.98 \text{ kg m}^{-3}$ per decade) consistent with the large-scale trend in the reanalysis seen in Fig. 6a. At WUHN (Fig. 8b), the GPS trend estimate is positive (0.34 kg m^{-3} per decade) while the ERA-Interim estimate is negative (-1.45 kg m^{-3} per decade). The IWV difference time series shows several breaks (in 1999, 2005 and at the end of 2006) though none of them coincides with known GPS equipment changes. In fact, the break at the end of 2006 is associated with the change in radiosonde from the Shang-M to Shang-E, which is assimilated by ERA-Interim (Wang and Zhang, 2008). Zhao et al. (2012) found that prior to this change there was a 2 kg m^{-3} wet bias in the radiosonde data at the Wuhan station, in comparison with GPS. This moist bias is also observed in ERA-Interim prior to the end of 2006. This case will be further discussed below when trends from MERRA-2 reanalysis are analysed (Section 5). At SHAO and CRO1, and a few other sites (e.g. SYOG, DARW, ANKR) inhomogeneity in the IWV difference series coincide with documented GPS equipment changes (not shown). Representativeness differences are suspected at some mountainous and coastal sites (e.g. AREQ, CFAG, KIT3, MAW1, SANT, SYOG and the other sites discussed in the previous section). Some sites show also more gradual drifts in the time series which don't seem connected with known GPS equipment changes (e.g. MAW1, Antarctica). At such sites, drifts in the reanalysis are plausible and will be further discussed below when MERRA-2 results are analysed.

Wang et al. (2016) studied nearly the same period (1995-2011) using radiosonde and GPS data over land and microwave (MWR) satellite data over oceans. Over the oceans, results that are significant in ERA-Interim are consistent (i.e. same sign) with those obtained by Wang et al. (2016), despite the fact that they are not always significant over land in the latter study. No results are obtained over most of Africa and the north-western part of South America due to a lack of data. The drying for north-eastern Africa and moistening over central Africa and north-western South America are therefore not confirmed by the Wang et al. (2016) study. For the other continental areas with weaker trends, results are not always in agreement, for instance over central Asia, where a moistening trend is generally observed in Wang et al. (2016). The western part of USA presents a strong spatial variability in both studies but results are generally not consistent locally. Greenland trends also present opposite signs. When comparing with the GPS results obtained by Wang et al. (2016), there is a general sign agreement, with some different sign trends in central Australia (ALIC station) and Iceland (REYK). These differences may be due to the extra year in their analysis (as differences in the beginning and ending of time series have an impact on the trend estimation, especially when trends are of low intensity and not significant, and the period at study is relatively short).

Mis en forme : Couleur de police : Automatique, Anglais (Royaume-Uni)

Although the study does not concern the same period, Trenberth et al (2005) reported similar trend signs to ERA-interim over Africa and South America in the NVAP data (1988-2001) and positive trends over western Pacific, the Indian and Atlantic oceans with SSM/I data (1988-2003). As discussed above, differences are observed over Eastern Pacific where El Niño events strongly affect the trend estimates. Note also a difference in the sign of the trend over Australia (an area which will be discussed later). Wagner et al. (2006) studied the IWV trends in satellite observations from the Global Ozone Monitoring Experiment for the 1996-2002 period. Although their study period is short, they also found positive IWV trends over the western tropical Pacific Ocean and large parts of the southern oceans, and negative trends over North Africa. Over northern Australia, they found a negative trend, which is in agreement with what we obtain but not with Trenberth et al. (2005). This area is thus likely sensitive to the period at stake. The western part of the USA is also an area where differences between the studies are present, but it seems that spatial variability is strong and thus results strongly depend on the resolution of the datasets, and not only on the period. Thus, despite the different periods and the use of different observing systems, some areas show consistent trend signs with ERA-Interim which indicates that the results are likely robust. However, the trends obtained in our study can differ from those presented by other authors for other periods, as the trend estimation is dependent on the time period at study.

To better understand the trends, we separated them by seasons (DJF or JJA), which are presented in Figs. 9a and b, respectively.

A striking feature of the seasonal trends is their relatively larger magnitude compared to the monthly trends. Large changes in magnitude and/or sign are also noticeable in most regions. These features emphasize that atmospheric circulation (which is largely changing between seasons) plays an important role in IWV trends. Trends of opposite signs between winter and summer can be observed in western Antarctica, central South America, south Africa, eastern Europe and off the West coast of the USA. A strong drying occurs over Antarctica in JJA and over central Asia during JJA and DJF (though not exactly at the same location). Western Europe shows a drying in winter (DJF) and a moistening in summer, which explains the weak trend when considering the whole year. Over Australia, according to ERA-Interim, the drying is stronger in DJF, i.e. when associated with a decrease of the intensity of the moist flow during the monsoon period. The differences between our study and the one of Trenberth et al. (2005) are consistent with the theory that precipitation over western and northern Australia (the part of Australia mostly influenced by the monsoon flow in DJF) are strongly sensitive to the SST over the western central Pacific Ocean (10°S-10°N; 150°E-200°E) (Brown et al., 2016). In ERA-Interim and satellite observations by Wang et al. (2016), during 1995-2010, the SST over this part of ocean has increased (indicated by a moistening, according to C-C law), and is associated with a drying over Australia, while during 1988-2001, a strong drying is observed over the central-western Pacific Ocean, associated with a moistening over Australia. Another area likely sensitive to the intensity of the monsoon flow is northern Africa, where the drying is occurring in JJA over eastern Sahel, in a band covering Chad, Sudan and Eritrea.

Overall, the seasonal trends estimated from the GPS data confirm the features discussed above for ERA-Interim. The sites with largest differences in the seasonal estimates are also listed in Table 2. In addition to the sites where issues were noticed in the monthly trends, the list includes a few more sites which also show up in Figs. 9a and b (most notably KIRU in Sweden, COCO in the Indian Ocean, IRKT in Russia, and ANKR in Turkey). Trend estimates at some of these sites might be inaccurate due to the enhanced impact of time gaps for the short seasonal time series (based on 16 years at best).

Mis en forme : Retrait : Première ligne : 0,5 cm

5 Trends in ERA-Interim and MERRA-2

5.1 Global analysis

In this section, MERRA-2 is inspected to complement ERA-Interim and GPS namely in regions of high uncertainty in these datasets (e.g. Antarctica) or in regions where few or no GPS data are available (e.g. Africa, Asia, the global oceans). The monthly IWV trends computed for MERRA-2 (Figs. 10a, b) show many of the same drying and moistening regions as ERA-Interim (Figs. 6a, b). They describe consistent global moistening/drying dipoles along the inter-tropical Pacific Ocean, across Australia, South America and between eastern and western USA, and general moistening over the Arctic and Europe. However, there appears to be also significant differences over several parts of the globe, in particular over Indonesia and the Indian Ocean, central Africa, western (coastal) and northern Africa, central Asia and Antarctica.

Over Antarctica, the monthly trends in MERRA-2 (Figs. 10a, b) are significantly positive, in opposition to what is seen in ERA-Interim (Figs. 6a, b). Over Antarctica, the monthly trends in MERRA-2 and GPS (Fig. 5b) are significantly positive, in opposition to what is seen in ERA-Interim (Fig. 5a) where the trends are mainly negative, especially in the interior of the continent. However, one can notice that ERA-Interim shows spotted areas of positive trends in the vicinity of the GPS stations which are in reasonable agreement with MERRA-2 and GPS. These locally positive trends in ERA-Interim might be explained by the influence of surface and/or upper air observations collected from these sites that are assimilated in this reanalysis. Comparing ERA-Interim and MERRA-2 IWV time series in the interior of the continent reveals that the reanalyses diverge mainly before year 2000, with a positive trend in MERRA-2 between 1995 and 2000 (not shown). This divergence might be explained by a combination of differences in the observations actually assimilated and differences in the assimilation systems. Observations in the interior of the continent are most likely from satellites only. General documentation indicates that both reanalyses use the same types of satellite observations globally (Dee et al., 2011; Gelaro et al., 2017). However, their assimilation over the Antarctica's ice sheet may differ between the reanalyses. It is not said whether or not these in the documentation how much of the data are actually assimilated over Antarctica. This kind of information can only be checked from assimilation feedback statistics.

Over central/east Asia, and over northern South America, ERA-Interim and MERRA-2 trends also disagree. The GPS data are in better agreement with MERRA-2 in the former region and with ERA-Interim in the latter.

Figure 6 shows the seasonal trends. A striking feature seen in both reanalyses is their relatively larger magnitude compared to the monthly trends (Fig. 5). Large changes in magnitude and/or sign are also noticeable in most regions between seasons. These features emphasize that atmospheric circulation (which is largely changing between seasons) plays an important role in IWV trends.

In DJF (Fig. 6a, b), the agreement between reanalyses is surprisingly good, given the inconsistencies pointed out from the monthly trends. The agreement of the reanalysis with GPS is also quite good, though some GPS trends are in strong contradiction (e.g. at IRKT in Siberia, KIRU in Sweden, IISC in India, and COCO east of Indonesia which have very large magnitudes). Over Antarctica, the drying/moistening east/west dipole is consistent in both reanalyses though they are of

Mis en forme : Retrait : Première ligne : 0,5 cm

different magnitudes. A drying/moistening dipole is also seen across Australia, consistent with the theory that precipitation over north-western Australia (the part of Australia mostly influenced by the monsoon flow in DJF) is very sensitive to the SST pattern over the western central Pacific Ocean (10 °S-10 °N; 150 °E-200 °E) (Brown et al., 2016). Over Indonesia and the Maritime Continent ERA-Interim trends are positive while MERRA-2 trends are negative. Comparing IWV time-series in the central part of this region reveals that though they are well correlated ($r = 0.89$), MERRA-2 shows a larger seasonal cycle than ERA-Interim (not shown). GPS observations are only available at the outer bound of the domain where both reanalyses are in better agreement with each other and also with GPS except for station CCJM where GPS has a large discontinuity. Another exception is station GUAM (14 °N, 145 °E), where GPS is in agreement with ERA-Interim while MERRA-2 has opposite trends. ERA-Interim and MERRA-2 trends also disagree in several places in central Asia, namely in China where GPS data are in better agreement with MERRA-2 (stations WUHN and SHAO), and in northern and central Africa (but no GPS data are available there). The moistening trend over northern South America is seen in both reanalyses but is less intense in MERRA-2. However, GPS trends at stations KOUR and BRAZ are in better agreement with ERA-Interim.

The seasonal trends computed from MERRA-2 (Figs. 10c, d) are in better agreement, in terms of moistening/drying patterns, with ERA-Interim and GPS in DJF than in JJA. In DJF, the east-west dipole in the trends over Antarctica seen in ERA-Interim is confirmed by MERRA-2 (though the intensities are different), as well as the strong drying trend over Siberia, the Arabian peninsula, western Australia, western Europe, and most of the USA; and the strong moistening over the Arctic. In JJA, on the other hand, we can find many differences between the two reanalyses which were already noticed in the monthly trends. Opposite trends are seen in Indonesia and in most of south Asia, north and central Africa, Antarctica, but also in the eastern Arctic region.

Over Antarctica, the seasonal trends at the GPS stations are more consistent with MERRA-2 than with ERA-Interim in both seasons (Figs. 10c, d), though the GPS trends have a positive bias because of a processing inhomogeneity already mentioned. Interestingly, in JJA the contrasted trends with different signs seen in the GPS data (positive around SYOG, MAW1 and MCM4, and negative around DAV1 and CAS1) are well reproduced by MERRA-2, whereas the ERA-Interim trends are negative throughout.

Over Europe and Middle East, the contrasted trends between seasons seen in ERA-Interim (Figs. 6c, d) are confirmed with MERRA-2 (Figs. 10c, d) and are in accordance with GPS data at many sites, except at a few sites where GPS trends are opposite to both reanalyses, mainly: at KIRU (Sweden), IRKT (Russia), ANKR (Turkey). Opposite trends are also observed at other GPS sites over Scandinavia, namely at METS and SVTL (Finland) and ONSA (Sweden).

Over northern Africa, the two reanalyses show similar trend patterns in DJF, though not perfectly collocated (e.g. a tongue of negative trend is extending across western Sahel in ERA-Interim whereas in MERRA-2 it is more limited to the western countries: Senegal, Mauritania, and western Mali). In JJA, on the other hand, the strong drying already highlighted in ERA-Interim which extends over most of north Africa is almost absent in MERRA-2 where most of northern Africa is seen as moistening. This striking difference emphasizes the uncertainty of reanalyses in this data sparse region as also noticed by Bauer, 2009, and Karbou et al., 2010.

During the 1995-2010 period, this SST pattern has actually been warming and the atmosphere moistening, leading to a drying over north-western Australia (Wang et al., 2016).

In JJA (Fig. 6c, d), the conclusions are more contrasted. Though the reanalyses agree generally well over the oceans, except over the Maritime Continent, the trends over land are poorly consistent over most continents (Asia, Africa, South America, and Antarctica). Over these regions, the GPS trends are generally in better agreement with MERRA-2. Over northern Africa, the drying in ERA-Interim is in contradiction with the recent recovering of precipitation over West Africa (Sanogo et al., 2015). In this respect, the MERRA-2 trends are more realistic.

4 Long-term IWV trends in the reanalyses (1980-2016)

4.1 Global analysis

Interpretation of IWV trends of the previous section must be tempered by the fact that the time series used here are relatively done cautiously as the trends have been estimated for a specific and rather short. Indeed, period of 15 years (from 1995-2010). They should thus not be considered as representative of a longer period and might also be impacted by decadal variability and/or large singular events such as El Niño. Trenberth et al. (2005) argued that the dominance of the 1997-98 El Niño event suggests that a longer time series may be required to obtain fully stable patterns of linear trends. The number of years needed to obtain a statistically significant trend in IWV in some regions, given its high variability, may never be achieved. In order to assess how consistent our trends obtained for the 1995-2010 period (when GPS data are available) are with longer-term trends, we computed them for the full length common to ERA-Interim and MERRA-2 (1980-2016).

Figure 7 shows the monthly trends for both reanalyses over the period 1980-2016. In both reanalyses most structures in ERA-Interim are similar to those seen for the short period (Fig. 6a) and the long (Fig. 11a) period, although the intensities are generally weaker for the longer period (note that the colour bars are different for Figs. 6 and 11), but most of them are significant. Over land in ERA-Interim, the drying and moistening trends over Africa and South America show similar patterns, as well as the moistening trends over eastern and northern regions of Europe and the drying trends over Antarctica. The main differences between periods (changes in sign of the trends) appear over the eastern tropical Pacific, Canada, the Arabic Peninsula, the region around Madagascar, Western Australia, Mexico, and a small part of Antarctica. The drying trend over Australia observed for the shorter 1995-2010 period is not observed in the long term. For this longer period, trends are mostly not statistically significant, which suggests that there might have been periods of moistening trends as part of decadal variability during the 1980-2016 period. These changes are seen in MERRA-2 as well, which gives good confidence that they are due to decadal variability in the global and regional climates. However, the main differences between reanalyses already highlighted for the short period remain (over Antarctica and the global southern oceans, northern Africa, and eastern Asia) except over the Maritime Continent where MERRA-2 now represents a moistening trend before the drying trend. Over the oceans, an overall moistening trend (except a strong drying off the coast of Antarctica) consistent with ERA-Interim and over Australia where the reanalyses now disagree.

Figure 8 shows the seasonal IWV trends and temperature trends. It is observed, especially in the northern hemisphere, seen that over the oceans, the temperature trends have generally the same sign as the IWV trends (but several areas show different patterns for both periods. For the Atlantic Ocean, a different sign is observed along the eastern coast of North America, with a significant moistening for the longer period, while a drying is confirmed by GPS around Bermuda for the shorter period. In the south, the drying trend is spatially more extended and statistically more significant for the longer period. Over the Indian ocean, for the short period, the western part moistens and the eastern part dries, and opposite trends are obtained over the longer period. Over the Pacific Ocean, even though the patterns look similar, the spatial variability is stronger for the shorter period, with a more intense moistening along the equator, and west of Patagonia and a weaker moistening around Alaska. Comparing the seasonal trends in ERA-Interim for both periods, the JJA patterns are mostly consistent over land and ocean between the two periods (Figs. 9b and 12g). Slight differences appear over India (where the moistening trend is more spatially extended in the longer period), Australia (where the trend is no longer significant), and Antarctica, where the drying trend is shifted eastward. For DJF (Figs. 9a and 12c), stronger differences exist. While the moistening trend of the short period over northern South America, southern part of Africa, Central and northern Europe, western Canada and Alaska and Arctic are consistent with the longer period, the ones over Patagonia, part of China and Afghanistan, part of Antarctica and western Africa are no longer visible. The drying trends over Antarctica are extended to the entire continent for the longer period. The eastern USA that dries between 1995 and 2010 presents a moistening trend when considering the longer period. The strong drying obtained over Australia in DJF is mostly cancelled over the long period. Over the oceans, differences exist over the Indian Ocean, western Atlantic (along the east coast of USA), part of the south Atlantic and Pacific and mostly around Antarctica.

According to the colours, as expected by Clausius-Clapeyron (C-C) equation, it is expected that an increasing temperature trend corresponds to an increasing IWV trend, especially over the oceans where the source of humidity is infinite. In order to assess the link between temperature and IWV trends, the trends in the 2-meter temperature were computed (even if the use of 2-m temperature may not be the best proxy of temperature in C-C equation). Monthly and globally (not shown), over the oceans, the temperature and water vapour trends have the same sign theory, despite some small-scale differences. Over land, all areas show an increase in 2-m temperature, except the high latitudes of the southern hemisphere. This means that, except over Antarctica, the drying observed in the afore-mentioned areas does not follow Clausius-Clapeyron relation: C-C theory. However, when we consider each season separately, some areas indicate a cooling (Figs. 12a8a, e) consistent with a drying (Figs. 12c8c, g). This is observed over Antarctica and to a lesser extent over Central Asia in DJF. Over eastern Australia, and South Africa, however, a weak cooling is observed while a significant moistening has been computed. For JJA, all continental areas show a significant warming, with the exception of parts of Antarctica, and a small area over northern Australia, where a cooling is also displayed, albeit not significant. Thus the C-C scaling ratio is not a good proxy for humidity when considering seasonal and regional variabilities and trends due to the important role of dynamics which allow the advection of dry or wet air masses (e.g. over USA, South America, eastern Sahel, and South Africa in JJA).

Mis en forme : Retrait : Première ligne : 0,5 cm

Trends in MERRA-2 over the long period (Figs. 12d, h) present different trends from ERA-Interim (Figs. 12e, g) over some areas as seen previously for the short period. They result from both the uncertainties that exist when computing trends, and from the differences in the physics and dynamics of the two reanalyses.

It is evident from Figs. 11 and 12 confirm that MERRA-2 presents a more general moistening trend than ERA-Interim, (as already seen over the shorter period), especially in the southern hemisphere in DJF (Figs. 12e8c, d), and in both hemispheres in JJA (Figs. 12g8g, h). The main differences in the trends over the oceans appear all around Antarctica, and those over continental areas are observed over Africa (where trends are positive in the North and negative in central Africa in MERRA-2 and the opposite in ERA-Interim) and USA in JJA, over Australia in DJF and over Antarctica in both JJA and DJF. Over Africa and Antarctica, the important differences which exist between ERA-Interim and MERRA2 for both long and short term periods suggest that the physical processes are not well represented. These areas correspond to areas with very few observations available for data assimilation, reducing the constraint on the models. A more detailed investigation of the dynamics over Africa and Australia is presented in the following subsection next subsections.

Other regions, such as the Indo-Pacific region have different trends over the shorter period, but are in better agreement over the longer period. This is more obvious during JJA (although there are also differences in DJF) and can be explained by the strong variability that requires longer time series in order to obtain meaningful trends. The good agreement between reanalyses over this area is an important result regarding in view of the fact that CMIP5 (Coupled Model Intercomparison Project Phase 5) models have large biases over this region in present day Sea Surface Temperature, which has direct consequences on the future projection of precipitation over Australia (Brown et al., 2016; Grose et al., 2014). However, the link between IWV trends over these oceans and Australia is not that strong here, since over Australia, while reanalyses were in good agreement over the shorter period, the western part presents a significant moistening in MERRA-2 over the long period in DJF, and a weak and not statistically significant drying in ERA-Interim. This area is thus investigated in more details in the next subsection. This may suggest discontinuities in the reanalysis data (due to changes in the data assimilated) or an uncertainty in the computation of long-term trends (due to the presence of different sign shorter term trends during the longer period):2014) and more generally over tropical and subtropical climates. Two areas are investigated in more details in the next subsections because of the disagreement between both reanalyses over them: Australia in DJF and Africa in JJA.

54.2 Analysis over Western Australia

Figure 139 displays the time series of IWV and temperature anomalies for a box over Western Australia (15-30 °S, 115-135 °E, as shown in Fig. 1410) for both the short and long periods, for both the full time series and the DJF seasons.

For As can be observed in Figs. 9a, b, the 1995-2010 period, moisture trend is opposite for the long (moistening) and short (drying) periods, for both reanalyses show drying and warming monthly trends (Fig. 14b), with significant IWV trend in both, while the temperature trend is only significant in ERA-Interim. For the longer time period (Fig. 14a), on weakly warming. However, when focusing on DJF period (Figs. 9c, d), the contrary, the monthly IWV trends are positive (moistening) for both reanalyses on average over the box, but not significant for ERA-Interim, and the temperature trends are again positive but

Mis en forme : Retrait : Première ligne : 0,5 cm

Mis en forme : Titre 2

smaller, and again significant for ERA-Interim. For DJF, the trends are generally consistent with the monthly trends, but of larger magnitude (e.g. IWV trends about $-2.4 \text{ kg m}^{-2} \text{ decade}^{-1}$ for the short period) though not statistically significant. It is noticeable that the difference in the IWV trends differences between reanalyses comes from are enhanced when considering the fact that long period. ERA-Interim IWV indeed starts with higher anomalies than MERRA-2 until 1990, but and ends with lower anomalies after the late 2000s, so that the resulting trend is close to zero and not significant.

What is striking when looking at the full time series (Fig. 13a) is The different IWV trend estimates between the two periods is due to the existence of extreme cold and humid periods in both reanalyses after 1992, with a strong occurrence around the 2000s, which impact the linear trend estimate over the short period more strongly than over the long period. These periods correspond to DJF seasons 1997, 1999, 2000, 2001, 2006, and 2011 (Fig. 13c), (which starts in 1995) more strongly than over the long period. Power et al. (1998) and Hendon et al. (2007) have shown that during DJF the correlation between wetter years and colder years is strong at interannual time scales. For the longer period, the correlation between T and IWV is around $r = -0.55$ for both reanalyses, while for the shorter period it is higher at $r = -0.78$ for ERA-Interim and $r = -0.73$ for MERRA-2. However, there is also a more complex interaction between temperature, IWV and precipitation in this region, with studies over Australia concluding that dynamics mostly explain the variability and trend of temperature and precipitation.

The wetter and colder summers (correlation between T and IWV being around $-0.7/-0.8$ for both reanalyses over the short period) are associated with a dynamical anomaly (not shown), with a weaker wind and a switching direction on average in the box shown in Fig. 10. As can be seen in Fig. 10 over this box, in DJF, the southern part of the box is under the influence of south-easterly wind, while the northern part of the box indicates the penetration of maritime air mass coming from the north/northwest, and corresponding to the monsoon flow. The trend of the wind components in this box (indicated by the contours) show a reinforcement of the south-easterly wind to the detriment of the northern/ north-western flow. The cold and wet years occurring at the beginning of the period are thus associated with a stronger monsoon flow which attenuates at the end of the period. Hence, as already mentioned by several studies (e.g. Power et al. Consequently, we consider the wind at 925 hPa to assess the role of dynamics in these trends and variability. Figure 14 presents the mean zonal (u_{925}) and meridional (v_{925}) components of the wind, superposed by the trends of each component in contours. The mean states in u_{925} and v_{925} are similar in both reanalyses. The zonal components show mainly an easterly wind in the latitude band between 30°S and 5°S throughout the year (Figs. 14a, b), slightly reduced at its northern border during DJF where the wind turns westerly (Figs. 14 e, f). The mean meridional component is southerly over Australia (Figs. 14c, d) with a changing direction at its northern border during DJF (Figs. 14 g, h) leading to a convergence within the box in DJF. The convergence is roughly from north-east in the northern part of the box and from south-east in the southern part.

The trends show a reinforcement of the mean easterly component in the box in both reanalyses (Figs. 14a, b). In DJF, the easterly flow in ERA-Interim is increasing at the eastern border of the box and over central Australia while it is decreasing at the western border and over eastern Indian Ocean, hence explaining at least partly the drying and warming trend over the box (Fig. 13d). The trends in the mean meridional component are positive though quite weak in both reanalyses (Figs. 14c, d), thus

Mis en forme : Retrait : Première ligne : 0,5 cm

indicating a strengthening of the mean southerly flow. During DJF, the meridional trend is very small in ERA-Interim while it is slightly positive again in MERRA-2.

Figure 15 displays the time series of wind vectors over the same box as Fig. 14. Figure 15a shows that the mean wind direction does not change much over the year, though the strength is slightly larger in the summer season (from January to March) due to an increase in the easterly component. The interannual variability is quite marked, both in DJF (Fig. 15b) and JJA (Fig. 15c). It is clear that the anomalously moister summers seen in Fig. 13 are associated with a dynamical anomaly, with a weaker wind, and a direction-switching from south easterly to easterly. The amplitude of wind direction difference is stronger in MERRA-2 than in ERA-Interim but both reanalyses are consistent.

(1998); Hendon et al. (2007)) dynamics mostly explain the variability and trends of temperature and humidity over this area.

Note that although the climatological means of zonal and meridional wind components are similar between ERA-Interim and MERRA-2, their trends over and around Australia present different patterns (Fig. 10), likely explaining the different IWV trends between both reanalyses.

4.3 Analysis over North Africa/eastern Sahel

Here we focus on a box over the eastern Sahel (10-20 °N, 10-40 °E). The monthly trend in IWV is negative (drying) and significant in both reanalyses (except for MERRA-2 for the longer period), though it is twice as intense in ERA-Interim than in MERRA-2 (Fig. 16b11b). Similarly, the temperature trends are positive (warming) and significant in both reanalyses. Over the long period, the IWV trend in MERRA-2 is close to zero and not significant while that of ERA-Interim is still significantly negative, while the temperature trends are again positive (Fig. 16a). Though the monthly anomalies show many similarities, their agreement is not as good as seen for the box over Australia far from being perfect. The general strong negative IWV trend in ERA-Interim implies that IWV anomalies are higher in ERA-Interim at the beginning of the period and lower at the end of the period. However, both reanalyses present four different periods in the time IWV series: a drying trend at the very beginning (1980-1985) followed by a moistening trend until 1995, then followed by a new drying period lasting until around 2008 when the trend seems to stop. As a consequence, over the shorter period, both reanalyses show a significant monthly drying, even though for ERA-Interim the IWV trend is twice as intense (Fig. 16b (Fig. 11a,b)).

As observed for IWV anomalies, the trend in T anomalies also stops at around 2008 (Fig. 16a11a). Before that period, the temperature anomaly is increasing significantly, despite strong month-to-month variability. However, there is low/negative correlation appears between IWV and T anomalies when considering full the monthly time series (Fig. 16a). For the longer period, the correlation between T and IWV is close to zero for MERRA-2 and about $r = -0.31$ for ERA-Interim, while for the shorter period it is higher at $r = -0.41$ for ERA-Interim and $r = -0.29$ for MERRA-2. In JJA, the trends same periods of drying/moistening are strong and go on after 2008 observed (Fig. 16e11c). The correlation of anomalies for JJA between both reanalyses is quite good, both for IWV (around $r = 0.67$ for the short period and $r = 0.63$ for the longer period) and T (around $r = 0.69$ for both periods), although their amplitudes and trends are quite different. MERRA-2 presents an overall moistening

Mis en forme : Titre 2

Mis en forme : Retrait : Première ligne : 0,5 cm

trend in JJA over the long period, while ERA-Interim shows a drying (Fig. 16e). IWV trends in both reanalyses are significant but of opposite signs, while 8g, h and 11c). Simultaneously, the temperature trends are both positive and significant. Over the short period (Fig. 16d), the IWV trend in MERRA-2 becomes close to zero while the other trends remain consistent with the longer period. Over the short period, the IWV trend in JJA in MERRA-2 is close to zero while it is still strongly negative in ERA-Interim (Fig. 16d). The relation between IWV and temperature trends in this arid region is, thus not expected to follow explaining the IWV trends according to C-C relationship and IWV especially is expected to be more related to changes in the atmospheric circulation.

The zonal and meridional wind components Dynamics at 925hPa over the short period are shown in Fig. 17. 12. The mean states are plotted in colours over which the contours of the trends are superposed. The mean states in u925 and v925 are similar in both reanalyses, with a mean monthly north-easterly wind over the box (Figs. 17a12a, b, c, d) which is almost completely replaced with a south-westerly wind in JJA (Figs. 17e12e, f, g, h). This wind is slightly stronger in ERA-Interim than in MERRA-2. For both reanalyses, the trends in the mean flow indicate an increase in the zonal component (Figs. 17a12a, b). The trends in the meridional wind component show a dominant increase in the northerly from the Sahara. This trend may explain the general warming and drying in the eastern Sahel. The trends differ, however, with MERRA-2 showing a decrease in the northerly flow in upper-left angle of the box (Fig. 17d12d) while ERA-Interim shows an increase there and an increasing southerly inflow at the southern border of the box (Fig. 17e12e). This difference can explain the difference of intensity in these trends. In JJA, the trends in MERRA-2 are very weak (Figs. 17f12f, h) while in ERA-Interim there is a strong increasing of the southerly flow from the Central Africa and of the north-easterly flow from the Sahara, explaining the net drying and warming (Fig. 16d-11d). Figure 13 displays the interannual variability of JJA wind (monsoon flow) averaged over the box for both reanalyses.

The monthly mean time series of the wind in the box (Fig. 18a) clearly indicates the time of the monsoon onset (May), when the wind shifts from north easterly to south westerly and retreat (September). This monsoon flow appears stronger in ERA-Interim than in MERRA-2, while the flow in the dry season is stronger in MERRA-2 (see also Figs. 18b and c). From the time series of JJA wind vectors (Fig. 18b) it is clear that ERA-Interim has a stronger southerly flow in JJA and weaker northerly flow for the other months (Fig. 13a) with large interannual and decadal variability. (Fig. 13b). The time series of wind in JJA in MERRA-2 clearly indicates the same four periods than for the IWV trends identified above, with a weakening of the south-westerly wind between 1980 and 1985, followed by an intensification of the monsoon flow arriving in this box between 1985 and 1995, and a wind decreasing and turning to the west until 2005 or 2006 and then becoming more stable on average. In ERA-Interim, we only observe two main periods: a weaker south/south-westerly wind at the beginning of the period followed by an intensification after 1990. The wind intensity is maximum between 1995 and 2000 but stays quite intense and with a south/south-westerly direction until the end of the period, being stronger and more southerly than in MERRA-2 after 2000. The different dynamics of the two reanalyses observed in this box partly explains the increasing deviation between both reanalyses at the end of the period.

65 Summary and conclusions

Atmospheric reanalyses play an important role in the global climate change assessment and their accuracy has significantly improved in recent years. In this study we investigated the means, variability, and trends in two modern reanalyses (ERA-Interim and MERRA-2). The means and variability in IWV in the reanalyses were inter-compared and compared to ground-based GPS data for the ~~period 1995-2010. The global distribution of IWV in ERA-Interim and GPS is remarkably consistent, even in regions of strong gradients, where IWV varies strongly. However, 1995-2010 period.~~ ERA-Interim was shown to exhibit a slight moist bias in the extra-tropics ($\sim 0.5 \text{ kg m}^{-2}$) and a slight dry bias in the tropics (~~also found in comparison with relation to both GPS and MERRA-2~~), which is consistent with other studies (e.g. Trenberth et al., 2011). Inter-annual variability in ERA-Interim is highly consistent with GPS ~~and is dominated by ENSO with variations as large as 20% IWV in DJF in the tropics, and in the mid to high northern latitudes.~~ good agreement with MERRA-2. Differences were pointed out between GPS and ~~ERA-Interim reanalyses~~ at only a few stations, mostly located in coastal regions and regions of complex topography, where representativeness errors put a limit to the comparison of gridded reanalysis data and point observations.

Previous studies have concluded that during recent decades IWV has increased with time both over land and ocean regardless of the time period and dataset analysed, except for some of the older reanalyses and/or some inhomogeneous observational datasets (Trenberth et al., 2005; Dessler and Davis, 2010; Bock et al., 2014; Schröder et al., 2016; Wang et al. 2016). Nevertheless, most global atmospheric reanalyses still have substantial limitations in representing decadal variability and trends in the water cycle components because of assimilation increments and observing system changes (Trenberth et al., 2011). In this study we found that trends in IWV and surface temperature in ERA-Interim and MERRA-2 are fairly consistent, with positive IWV trends generally correlated with surface warming over most of the tropical oceans, as well as the Arctic, part of North America, Europe, and the Amazon. However, significant differences are found as well over several parts of the globe, with MERRA-2 presenting a more general global moistening trend compared to ERA-Interim. The most striking uncertainties are seen over Antarctica and most of the southern hemisphere, especially during JJA, where IWV trends are often of opposite signs, but also over most of central and northern Africa, as well as ~~Indonesia, the Indian Ocean, Maritime Continent and central/eastern~~ Asia. The discrepancies are observed for both the extended common time record (1980-2016) and for the shorter time period (1995-2010) when GPS data are available. Over the latter period, the GPS IWV data point to a large erroneous negative (drying) trend in ERA-Interim over Antarctica ~~and over north-eastern Africa in JJA. The comparison with MERRA-2 indicates that both reanalyses have actually problems over north Africa.~~ Few in-situ observations are available for assimilation in ~~this region~~ ~~both regions~~ and the spurious trends in ERA-Interim might be due to model biases and changes and in the assimilated satellite data (Dee et al., 2011). Further investigation using assimilation feedback statistics and satellite IWV observations would help to better understand the origin of biases and spurious trends in ~~this region~~ ~~these regions~~. In most other regions, the trends in ERA-Interim have the same sign but different magnitudes than GPS, with positive biases in the tropics and negative biases in the higher northern latitudes.

Mis en forme : Titre 1

Mis en forme : Retrait : Première ligne : 0,5 cm

Another distinct feature in ERA-Interim is the unphysically strong summer (JJA) negative IWV trend over north-eastern Africa. The absence of long-term GPS records over this region prevents us from its direct assessment. The comparison with MERRA-2 indicates that both reanalyses have problems over Sahel and Sahara. This is actually not surprising as very few in-situ observations are available in this region, and models are known to have large biases over this region. These biases are

The biases over Africa are likely associated with problems in representing some of the governing continental physical and dynamical processes, namely the dry convection in the Saharan heat low and moisture advections from the ocean (Meynadier et al., 2010). Variations in IWV and atmospheric circulation are strongly correlated in this arid region. This co-variability provides a reasonable explanation for the observed variability and decadal trends in each of the reanalyses and of the differences between them (e.g. stronger increase of the dry northerly flow in ERA-Interim). Here as well, assimilation feedback statistics might help to understand the origin of biases, and their link with atmospheric dynamics in this region.

A more detailed investigation of IWV, surface temperature, and atmospheric circulation was also presented for western Australia, which is in many aspects governed by similar atmospheric processes as northern Africa (dry continental convection associated with a heat low and summer monsoon). However, this region benefits from more direct in-situ observations, as well as moisture and surface wind observations over the ocean from space, which have a strong impact on moisture transport from the surrounding oceans to the continent. Hence it is not surprising that both reanalyses are in better agreement and closer to the observed GPS IWV trends there. Interestingly, the region is marked by positive trends in surface temperature and IWV for the longer period, consistently with the global warming, but with an opposite IWV trend for the shorter period. The time series of IWV anomalies and surface temperature show that strong interannual to decadal variability in IWV is again correlated with anomalies in atmospheric circulation with colder years being wetter.

Compared to past studies using older reanalyses, we find that modern reanalysis made significant improvements in the provide a better representation of IWV means and the strong interannual variability over the oceans and most continental areas. However, the weaker decadal variability and trends still suffer from large uncertainties in data-sparse regions such as Africa and Antarctica. More generally, model biases and changes in the observing system are still suspected, which prevent reanalyses produced with different models and assimilation systems from being consistent to better than about $\pm 10\%$ IWV per decade. It will be of special interest as future work to investigate ERA5, the new reanalysis from ECMWF, which benefits from many improvements compared to ERA-Interim (<https://software.ecmwf.int/wiki/pages/viewpage.action?pageId=74764925>).

An absolute assessment of the reanalyses could be made in this study using independent IWV data from the ground-based GPS network for the period 1995-2010. Even though the GPS data were produced using homogeneous reprocessing and quality checking, inhomogeneities due to equipment changes were evidenced for a small number of sites; see Appendix B). Homogenisation of the GPS dataset is currently being undertaken using different processing and modelling strategies as well as statistical homogenisation techniques that should help detection and correcting the biases and offsets. An extension of the dataset is also planned as a few more years of observations are now available for reprocessing.

Appendices

Appendix A: Comparison between methods of trend estimation

There are many methods used in the literature to estimate linear trends from geophysical data. Two of the most widely used are compared in this Appendix: the Theil-Sen method (after Theil, 1950, and Sen, 1968) which we used in the manuscript, and the Least Squares method (e.g.: Weatherhead et al., 1998). Both methods assume that the data time series, y_i , can be modelled by a linear function of time t_i of the form:

$$y_i = at_i + b + N_i \quad i = 1, \dots, n \quad (A1)$$

Where a and b are the unknown slope and intercept parameters to be estimated, and N_i is the random noise or error. The ordinary Least Squares Method (LSM) method determines the set of parameters \hat{a} and (\hat{a}, \hat{b}) that minimizes the sum of squared residuals given by:

$$\min_{(\hat{a}, \hat{b})} \sum_{i=1, n} [y_i - (\hat{a}t_i + \hat{b})]^2 \quad (A2)$$

More sophisticated variants are described in Rousseeuw and Leroy (2003) which include non-uniform weighting and models that take autocorrelation in the noise term into account whereas the ordinary LSM assume identically independent noise samples.

The Theil-Sen estimator method, as defined by Theil (1950), is a non-parametric method that determines the trend by computing the median of slopes of lines through all pairs of points in the time series:

$$\hat{a} = \text{med}_{1 \leq i < j \leq n} \frac{y_j - y_i}{t_j - t_i} \quad (A3)$$

Once and once the slope has been determined, the intercept is derived from $\hat{b} = \text{med}_{1 \leq i \leq n} y_i - \hat{a}t_i$. Sen (1968) extended the method to handle ties among the times (i.e. the case when two data points have the same time (so-called ties)).

Both We compared both methods were applied to the global ERA-Interim and GPS monthly mean IWV anomalies, obtained after the removal of the seasonal cycle as described in Section 2 of the paper, for the 1995-2010 period. The results are shown in Fig. A1.

The differences between trends obtained using the two methods for the ERAI data are shown in Fig. A1a. These differences are under $0.5 \text{ kg} \cdot \text{m}^{-2} \cdot \text{decade}^{-1}$ for most of the globe, except around the Equator, where the ordinary LSM Least Squares method overestimates the trends in the eastern Pacific Ocean and underestimates the trends in the western Pacific Ocean (Fig. A1a). Consistent results are observed from the GPS IWV anomalies including gaps in the times series as shown in Fig. A1b.

The time series and trends at two points over the regions with large opposite differences are shown in Figs Fig. A1c (eastern Pacific Ocean) and d Fig. A1d (Coco Island in the western Pacific Ocean). It is observed that the Theil-Sen method is less

Mis en forme : Titre 2, Interligne : simple

Mis en forme : Police :10 pt

Tableau mis en forme

Mis en forme : Police :10 pt

Mis en forme : Police :10 pt

Mis en forme : Police :10 pt

Mis en forme : Police :10 pt

Mis en forme : Police :10 pt

Mis en forme : Police :10 pt

Mis en forme : Police :10 pt

Mis en forme : Police :10 pt

Mis en forme : Police :10 pt

Tableau mis en forme

Mis en forme : Police :10 pt

Mis en forme : Police :10 pt

Mis en forme : Police :10 pt

Mis en forme : Police :10 pt

Mis en forme : Police :10 pt

Tableau mis en forme

Mis en forme : Retrait : Première ligne : 0,5 cm

affected by the strong positive anomalies observed in 1997/1998 in the tropical Pacific (due to a strong El Niño event), and at the end of the time series, in 2010, for the Coco Island GPS station.

~~The~~ In fact, the Theil-Sen estimator is known to be generally more robust than the Least Squares method (Rousseeuw and Leroy, 2003) and less sensible to the beginning and ending of the time-series (Wang et al., 2016), so this was the method chosen to estimate the trends analysed throughout the paper.

Mis en forme : Retrait : Première ligne : 0,5 cm

Appendix B: Detailed comparison between ERA-Interim and GPS at the GPS sites

B.1. Data and methods

The GPS and reanalyses don't agree at certain GPS sites. In this appendix we discuss in more detail the various causes for this, and especially those that originate from problems in the GPS data. In order to minimize the representativeness differences between the gridded reanalysis fields and the GPS point observations, a more elaborate intercomparison methodology is required. We used the ERA-Interim 6-hourly pressure level data (37 levels between 1000 and 1 hPa, among which 27 levels lie between 1000 and 100 hPa) from the 4 grid points surrounding each GPS station. For each grid point and time step, the IWV is recomputed by vertically integrating the specific humidity from the height of the GPS station to the top of the atmosphere (1 hPa). Most GPS station heights fall between two pressure levels, and the specific humidity at the station height can be interpolated from the adjacent levels. The reanalysis data are only extrapolated for stations located below 1000 hPa (the lowest pressure level). Interpolation and extrapolation are done linearly for specific humidity and temperature, and exponentially for pressure. The IWV at the location of the GPS stations is then obtained by a bilinear interpolation from the four IWV estimates. This approach provided more consistent reanalysis IWV estimates by comparison with the GPS data than any other approach that we tested (the GPS minus reanalysis differences are diminished at almost all sites with a few exceptions). The use of 6-hourly fields also allows time-matching of the GPS data before computing monthly averages, reducing temporal sampling issues.

B.2. Differences in the means and in interannual variability

The mean IWV differences between ERA-Interim and GPS are shown in Figs. B1a and B1b for all 104 GPS sites. At first glance, the results look very similar to those presented in Fig. 4a and 4b using a simplified comparison methodology.

The sites with most notable differences in the IWV means (ERA-Interim minus GPS) are: CFAG in the Andes cordillera with a bias of 6.5 kg.m⁻² (27 %) in DJF and 3.9 kg.m⁻² (43 %) in JJA and, SANT in Chile with -2.4 kg.m⁻² (-15 %) in DJF, and TSKB (in Japan) with 1.9 kg.m⁻² (24 %) in DJF. In JJA, four other sites have large biases: KIT3 in Uzbekistan with a value of 6.2 kg.m⁻² (35 %), POL2 in Kirghizstan with 3.2 kg.m⁻² (20 %), SYOG in Antarctica with 0.6 kg.m⁻² (32 %), and MAW1 in Antarctica with 0.4 kg.m⁻² (31 %). The inspection of the time series shows that at some of these stations the biases are not constant in time but contain large seasonal variations, such as e.g. at CFAG (Fig. B2a) or KIT3 (Fig. B2b). These sites are located in coastal regions and/or regions with complex topography. Although we used here a more elaborate spatial and

temporal matching of reanalysis and GPS data, representativeness errors can still be the cause of these biases. To investigate this point, we compared the (vertically adjusted) IWV values from all 4 grid points surrounding each GPS station to the bilinearly interpolated IWV value. We found that at CFAG, KIT3, POL2, SYOG, and MAW1, the bilinearly interpolated values did not minimize the IWV biases between the reanalysis and GPS. At these sites, the altitudes of the four grid points differ by more than 500m and the moisture profiles above are very different. In the case of SANT, although the interpolated value matches the GPS value better than any of the four surrounding grid point values, there is still a large bias explained by a variation in the altitude of the grid points of over 1500m.

Figures B1c and B1d show the differences of relative standard deviations between ERA-Interim and GPS. In JJA, the four stations with the largest differences (ERA-Interim – GPS) are located in Antarctica: MCM4, SYOG, MAW1, and DAV1 with differences of -39.7 % (p=0), -7.5 % (p=0.14), -4.6 % (p=0.21), and +4.1 % (p=0.17), respectively. In DJF, the largest differences are found for MKEA (Hawaii) and SYOG, where they amount to -11.5 % (p=0.33) and -4.7 % (p=0.13), respectively. In the case of SYOG, MAW1, and DAV1, representativeness errors are suspected again because of the large variability in the IWV values of the surrounding grid points connected with large variations in the altitudes (> 500m) of these grid points. In the case of MKEA, the variation in the altitude of the surrounding grid points is quite small because of the limited imprint of Mauna Kea Island on the 0.75° resolution grid of ERA-Interim. However, the difference in altitude between the GPS station and all four grid points is larger than 3000 m. In the case of MCM4 and SYOG, the inspection of the time series of monthly mean IWV and IWV differences (shown in Figs. B2c and d) reveals variations in the means which coincide with GPS equipment changes and processing changes and unexplained variations in the amplitude of the seasonal cycle resulting in a marked oscillation in the monthly mean differences (ERA-Interim – GPS). Variations in the means introduce a spurious component of variability in the GPS IWV series (e.g. in JJA, at MCM4 the standard deviation of GPS IWV is 56.9% compared to 17.2% for ERA-Interim).

B.3. Differences in trends

Inspection of Fig. 4a found a number of GPS stations where the trend estimates are large and of opposite sign compared to ERA-Interim: CCJM (south of the Japanese home islands), DARW (northern Australia), WUHN (eastern China), IRKT (central Russia), ANKR (Turkey), KOKB and MKEA (Hawaii), and MCM4 (Antarctica). Some of them (DARW, ANKR, KOKB, MKEA) are located in areas where the ERA-Interim trends change sign and a perfect spatial coincidence between the reanalysis and observations might not be expected. On the other hand, stations CCJM, WUHN, IRKT, and MCM4 are located within regions where the ERA-Interim trends are strong and significant, and extend over large areas. For some of these stations, the discrepancy is due to gaps and/or inhomogeneities in the GPS time series which corrupt the trend estimates.

Figs. B1e and f show the trend differences for the time-matched series. Compared to Fig. 4, the agreement is improved at DARW, ANKR and IRKT, and at many other sites (e.g. KELY in Greenland, SANT, MAW1). However, there are still many sites with large differences. The stations with largest differences are listed in Table B1.

Inspection of time series reveals the presence of large inhomogeneities at CCJM, MCM4 (see Fig. B2c), WUHN, SHAO, and CRO1. At CCJM (see Fig. B2e), the GPS minus ERA-Interim IWV difference time series has a large offset in 2001 which coincides with a GPS equipment change (receiver and antenna). This offset is responsible for a large negative trend estimate in the GPS series (-1.40 kg m^{-2} per decade) whereas the time-matched ERA-Interim series gives a positive trend ($+0.98 \text{ kg m}^{-2}$ per decade) consistent with the large-scale trend in the reanalysis seen in Fig. 4. At WUHN (Fig. B2f), the GPS trend estimate is positive (0.34 kg m^{-2} per decade) while the ERA-Interim estimate is negative (-1.45 kg m^{-2} per decade). The IWV difference time series shows several breaks (in 1999, 2005 and at the end of 2006) though none of them coincides with known GPS equipment changes. In fact, the break at the end of 2006 is associated with the change in radiosonde from the Shang-M to Shang-E, which is assimilated by ERA-Interim (Wang and Zhang, 2008). Zhao et al (2012) found that prior to this change there was a 2 kg m^{-2} wet bias in the radiosonde data at the Wuhan station, in comparison with GPS. This moist bias is also observed in ERA-Interim prior to the end of 2006. At SHAO and CRO1, and a few other sites (e.g. SYOG, DARW, ANKR) inhomogeneity in the IWV difference series coincide with documented GPS equipment changes (not shown). Representativeness differences are also suspected at some mountainous and coastal sites (e.g. AREQ, CFAG, KIT3, MAW1, SANT, SYOG and the other sites discussed in the previous section), while some sites show also more gradual drifts in the times series which don't seem connected with known GPS equipment changes (e.g. MAW1, Antarctica). At such sites, drifts in the reanalysis are plausible. Overall, the seasonal trends estimated from the GPS data confirm the trends found in ERA-Interim. The sites with largest differences in the seasonal estimates are also listed in Table B1. In addition to the sites where issues were noticed in the monthly trends, the list includes a few more sites which are also visible in Figs. 5a and b (most notably KIRU in Sweden, COCO in the Indian Ocean, IRKT in Russia, and ANKR in Turkey). Trend estimates at some of these sites might be inaccurate due to the enhanced impact of time gaps for the short seasonal time series (based on 16 years at best).

Mis en forme : Retrait : Première ligne : 0,5 cm

Mis en forme : Couleur de police : Automatique, Anglais (Royaume-Uni)

Acknowledgements. This work was developed in the framework of the VEGA project and supported by the CNRS program LEFE/INSU and ANR REMEMBER project (grant ANR-12-SENV-001). This work is a contribution to the European COST Action ES1206 GNSS4SWEC (GNSS for Severe Weather and Climate monitoring; http://www.cost.eu/COST_Actions/essem/ES1206) aiming at the development of the global GPS network for atmospheric research and climate change monitoring.

References

- Barnston, A. G., and Livezey, R. E.: Classification, seasonality and persistence of low frequency atmospheric circulation patterns, *Mon. Weather Rev.*, 115(6), 1083–1126, doi: 10.1175/1520-0493(1987)115<1083:CSAPOL>2.0.CO;2, 1987.
- Bauer, P.: 4D-Var assimilation of MERIS total column water-vapour retrievals over land, *Q. J. Roy. Meteor. Soc.*, 135: 1852–1862, doi:10.1002/qj.509, 2009.

Bock O, Keil C, Richard E, Flamant C, Bouin MN. Validation of precipitable water from ECMWF model analyses with GPS and radiosonde data during the MAP SOP. Q. J. R. Meteorol. Soc. 131:3013–3036, 2005.

Bock, O., Bouin, M. N., Walpersdorf, A., Lafore, J. P., Janicot, S., and Guichard, F.: Comparison of GPS precipitable water vapour to independent observations and Numerical Weather Prediction model reanalyses over Africa, Q. J. Roy. Meteor. Soc., 133, 2011-2027, doi: 10.1002/qj.185, 2007.

Bock, O., Willis, P., Wang, J., and Mears, C.: A high-quality, homogenized, global, long-term (1993–2008) DORIS precipitable water data set for climate monitoring and model verification, J. Geophys. Res. Atmos., 119(12), 7209-7230, doi: 10.1002/2013JD021124, 2014.

Bock, O., Bosser, P., Pacione, R., Nuret, M., Fourrié, N., and Parracho, A.: A high-quality reprocessed ground-based GPS dataset for atmospheric process studies, radiosonde and model evaluation, and reanalysis of HyMeX Special Observing Period, Q. J. Roy. Meteor. Soc., 142(S1), 56-71, doi: 10.1002/qj.2701, 2016.

Bosilovich, M.G., F.R. Robertson, L. Takacs, A. Molod, and D. Mocko: Atmospheric Water Balance and Variability in the MERRA-2 Reanalysis. J. Climate, 30, 1177–1196, <https://doi.org/10.1175/JCLI-D-16-0338.1>, 2017.

Brown, J. R., Moise, A. F., Colman, R., and Zhang, H.: Will a Warmer World Mean a Wetter or Drier Australian Monsoon?, J. Climate, 29(12), 4577-4596, doi: 10.1175/JCLI-D-15-0695.1, 2016.

Byun, S.H. and Bar-Server, Y. E.: A new type of troposphere zenith path delay product of the international GNSS service, J. Geodesy, 83(3-4), 367-373, doi: 10.1007/s00190-008-0288-8, 2009.

Chen, B. and Liu, Z.: Global water vapor variability and trend from the latest 36 year (1979 to 2014) data of ECMWF and NCEP reanalyses, radiosonde, GPS, and microwave satellite. J. Geophys. Res. Collins, M., An, S.I., Cai, W., Ganachaud, A., Guilyardi, E., Jin, F.F., Jochum, M., Lengaigne, M., Power, S., Timmermann, A., and Vecchi, G.: The impact of global warming on the tropical Pacific Ocean and El Niño, Nat. Geosci., 3(6), 391-397, doi:10.1038/ngeo868, 2010. Atmos., 121, 11,442–11,462, doi:10.1002/2016JD024917.

Dee, D. P. and Uppala, S.: Variational bias correction of satellite radiance data in the ERA-Interim reanalysis. Q.J.R. Meteorol. Soc., 135: 1830-1841. doi:10.1002/qj.493, 2009.

Dee, D.P., Uppala, S.M., Simmons, A.J., Berrisford, P., Poli, P., Kobayashi, S., Andrae, U., Balmaseda, M.A., Balsamo, G., Bauer, P., and Bechtold, P.: The ERA-Interim reanalysis: Configuration and performance of the data assimilation system, Q. J. Roy. Meteor. Soc., 137(656), 553-597, doi: 10.1002/qj.828, 2011.

Dessler, A. E., and Davis, S. M.: Trends in tropospheric humidity from reanalysis systems, J. Geophys. Res. Atmos., 115, D19127, doi: 10.1029/2010JD014192, 2010.

Gelaro, R., McCarty, W., Suárez, M.J., Todling, R., Molod, A., Takacs, L., Randles, C.A., Darmenov, A., Bosilovich, M.G., Reichle, R., and Wargan, K.: The modern-era retrospective analysis for research and applications, version 2 (MERRA-2), J. Climate, 30(14), 5419-5454, doi: 10.1175/JCLI-D-16-0758.1, 2017.

- Grose, M. R., Brown, J. N., Narsey, S., Brown, J. R., Murphy, B. F., Langlais, C., Gupta, A. S., Moise, A. F., and Irving, D. B.: Assessment of the CMIP5 global climate model simulations of the western tropical Pacific climate system and comparison to CMIP3. *International Journal of Climatology*, 34(12), 3382-3399, <https://doi.org/10.1002/joc.3916>, 2014
- Hamed, K. H., and Rao, A. R.: A modified Mann-Kendall trend test for autocorrelated data, *J. Hydrol.*, 204(1-4), 182-196, doi: 10.1016/S0022-1694(97)00125-X, 1998.
- Held, I. M., and Soden, B. J.: Robust responses of the hydrological cycle to global warming, *J. Climate*, 19(21), 5686-5699, doi: 10.1175/JCLI3990.1, 2006.
- Hendon, H. H., Thompson, D. W. J., Wheeler, and M. C.: Australian Rainfall and Surface Temperature Variations Associated with the Southern Hemisphere Annular Mode, *J. Climate*, Vol. 20 Issue 11, p2452-2467, doi: 10.1175/JCLI4134.1, 2007.
- IGSMAIL-6298, Reprocessed IGS Trop Product now available with Gradients, by Yoaz Bar-Sever, 11 Nov 2012, <http://igsceb.jpl.nasa.gov/pipermail/igsmail/2010/007488.html>.
- Karbou, F., Rabier, F., Lafore, J.-P., Redelsperger, J. L., and Bock, O.: Global 4D-Var assimilation and forecast experiments using land surface emissivities from AMSU-A and AMSU-B. Part-II: Impact of adding surface channels on the African Monsoon during AMMA, *Weather Forecast*, 25, 20-36, doi:10.1175/2009WAF222244.1, 2010.
- Kondratiev, K. Y.: *Radiation Processes in the Atmosphere* (Geneva: World Meteorological Organization), 1972.
- Lorenc, A. C.: Analysis methods for numerical weather prediction, *Q. J. Roy. Meteor. Soc.*, 112: 1177–1194, doi:10.1002/qj.49711247414, 1986.
- Mears, C. A., Wang, J., Smith, D., and Wentz, F. J.: Intercomparison of total precipitable water measurements made by satellite-borne microwave radiometers and ground-based GPS instruments. *J. Geophys. Res. Atmos.*, 120, 2492–2504. doi: 10.1002/2014JD022694, 2015.
- Meynadier, R., Bock, O., Gervois, S., Guichard, F., Redelsperger, J.-L., Agustí-Panareda, A., and Beljaars, A.: West African Monsoon water cycle: 2. Assessment of numerical weather prediction water budgets, *J. Geophys. Res.*, 115, D19107, doi:10.1029/2010JD013919, 2010.
- Mieruch, S., Schröder, M., Noël, S., and Schulz, J.: Comparison of decadal global water vapour changes derived from independent satellite time series, *J. Geophys. Res. Atmos.*, 119(22), 12489-12499, doi: 10.1002/2014JD021588, 2014.
- Ning, T., Wickert, J., Deng, Z., Heise, S., Dick, G., Vey, S., and Schöne, T.: Homogenized time series of the atmospheric water vapour content obtained from the GNSS reprocessed data, *J. Climate*, 29(7), 2443-2456, doi: 10.1175/JCLI-D-15-0158.1, 2016.
- O’Gorman, P. A. and Muller, C. J.: How closely do changes in surface and column water vapor follow Clausius–Clapeyron scaling in climate-change simulations? *Environ. Res. Lett.* 5, 025207, 2010.
- Power, S., Tseitkin, F., Torok, S., Lavery, B., and McAvaney, B.: Australian temperature, Australian rainfall, and the Southern Oscillation, 1910–1996: Coherent variability and recent changes, *Aust. Meteorol. Mag.*, 47, 85–101, 1998.

- Robertson, F.R., Bosilovich, M.G., Roberts, J.B., Reichle, R.H., Adler, R., Ricciardulli, L., Berg, W., and Huffman, G.J.: Consistency of Estimated Global Water Cycle Variations over the Satellite Era. *J. Climate*, 27, 6135–6154, <https://doi.org/10.1175/JCLI-D-13-00384.1>, 2014.
- Rousseeuw, P. J. and Leroy, A. M.: Robust Regression and Outlier Detection, Wiley Series in Probability and Mathematical Statistics, 516, Wiley, p. 67, 2003. ISBN 978-0-471-48855-2.
- Sanogo, S., Fink, A.H., Omotosho, J. A., Ba, A., Redl, R. and Ermert, V. (2015), Spatio-temporal characteristics of the recent rainfall recovery in West Africa. *Int. J. Climatol.*, 35: 4589-4605. doi:10.1002/joc.4309 Schröder, M., Lockhoff, M., Forsythe, J. M., Cronk, H. Q., Vonder Haar, T. H., and Bennartz, R.: The GEWEX Water Vapour Assessment: Results from Intercomparison, Trend, and Homogeneity Analysis of Total Column Water Vapour, *J. Appl. Meteorol. Clim.*, 55(7), 1633-1649, doi: 10.1175/JAMC-D-15-0304.1, 2016.
- Schneider, T., O’Gorman, P. A., and Levine, X. J.: Water vapor and the dynamics of climate changes, *Rev. Geophys.*, 48, RG3001, doi:10.1029/2009RG000302, 2010.
- Sen, P. K.: Estimates of the regression coefficient based on Kendall’s tau, *J. Am. Stat. Assoc.*, 63 (324): 1379–1389, JSTOR 2285891, MR 0258201, doi:10.2307/2285891, 1968.
- Sherwood, S. C., Roca, R., Weckwerth, T. M., and Andronova, N. G.: Tropospheric water vapor, convection, and climate, *Rev. Geophys.*, 48, RG2001, doi:10.1029/2009RG000301, 2010.
- Theil, H.: A rank-invariant method of linear and polynomial regression analysis, I, II, III, *Nederl. Akad. Wetensch., Proc.*, 53: 386–392, 521–525, 1397–1412, MR 0036489, doi: 10.1007/978-94-011-2546-8_20, 1950.
- Thorne, P.W. and Vose, R.S.: Reanalyses Suitable for Characterizing Long-Term Trends. *Bull. Amer. Meteor. Soc.*, 91, 353–362, <https://doi.org/10.1175/2009BAMS2858.1>, 2010.
- Trenberth, K. E., Fasullo, J., and Smith, L.: Trends and variability in column-integrated atmospheric water vapour, *Clim. Dynam.*, 24(7-8), 741-758, doi: 10.1007/s00382-005-0017-4, 2005.
- Trenberth, K.E., Fasullo, J.T., and Mackaro, J.: Atmospheric Moisture Transports from Ocean to Land and Global Energy Flows in Reanalyses. *J. Climate*, 24, 4907–4924, <https://doi.org/10.1175/2011JCLI4171.1>, 2011.
- Vey, S., Dietrich, R., Fritsche, M., Rülke, A., Steigenberger, P., and Rothacher, M.: On the homogeneity and interpretation of precipitable water time series derived from global GPS observations, *J. Geophys. Res. Atmos.*, 114, D10101, doi: 10.1029/2008JD010415, 2009.
- ~~Visbeck, M. H., Hurrell, J. W., Polvani, L., and Cullen, H. M.: The North Atlantic Oscillation: past, present, and future. Proceedings of the National Academy of Sciences, 98(23), 12876–12877, <https://doi.org/10.1073/pnas.231391598>, 2001.~~
- Wagner, T., Beirle, S., Grzegorski, M., and Platt, U.: Global trends (1996–2003) of total column precipitable water observed by Global Ozone Monitoring Experiment (GOME) on ERS-2 and their relation to near-surface temperature, *J. Geophys. Res. Atmos.*, 111, D12102, doi: 10.1029/2005JD006523, 2006.
- Wang, J., Zhang, L., and Dai A.: Global estimates of water-vapour-weighted mean temperature of the atmosphere for GPS applications, *J. Geophys. Res.*, 110, D21101, doi:10.1029/2005JD006215, 2005.

Wang, J., and Zhang, L.: Systematic errors in global radiosonde precipitable water data from comparisons with ground-based GPS measurements. *J. Climate*, 21(10), 2218-2238, <https://doi.org/10.1175/2007JCLI1944.1>, 2008.

Wang, J., Dai, A., and Mears, C.: Global Water Vapour Trend from 1988 to 2011 and Its Diurnal Asymmetry Based on GPS, Radiosonde, and Microwave Satellite Measurements, *J. Climate*, 29(14), 5205-5222, doi: 10.1175/JCLI-D-15-0485.1, 2016.

Weatherhead, E. C., Reinsel, G. C., Tiao, G. C., Meng, X. L., Choi, D., Cheang, W. K., Keller, T., DeLuisi, J., Wuebbles, D. J., Kerr, J. B., Miller, A. J., Oltmans, S. J., and Frederick, J. E.: Factors affecting the detection of trends: Statistical considerations and applications to environmental data, *J. Geophys. Res. Atmos.*, 103(D14), 17149-17161, doi : 10.1029/98JD00995, 1998.

~~Wolter, K., and Timlin, M. S.: Monitoring ENSO in COADS with a seasonally adjusted principal component index, In Proc- of the 17th Climate Diagnostics Workshop (Vol. 5257), 1993.~~

~~Wolter, K., and Timlin, M. S.: Measuring the strength of ENSO events: How does 1997/98 rank?, *Weather*, 53(9), 315-324, doi: 10.1002/j.1477-8696.1998.tb06408.x, 1998.~~

Zhao, T., Dai, A., and Wang, J.: Trends in tropospheric humidity from 1970 to 2008 over China from a homogenized radiosonde dataset *J. Climate*, 25(13), 4549-4567, <https://doi.org/10.1175/JCLI-D-11-00557.1>, 2012.

5

Table 2: Stations with most intense trend differences (ERA-Interim—GPS) computed from time-matched GPS and ERA-Interim IWV series.

[illegible]

Tr.diff > 1 kg.m ⁻³ .decade ⁻¹	CCJM	CCJM, DARW, GUAM, LPGS, COCO, SANT	CCJM, POL2
Tr.diff < -7 %.decade ⁻¹ (*)	MCM4, MAW1, PIN1	IRKT, POL2, PIN1, WUHN, YELL, WSLR	MCM4, MAW1, SYOG
Tr.diff > 7 %.decade ⁻¹ (*)	CCJM	CCJM, KIRU	AREQ

Mis en forme : Gauche, Espace Après : 8 pt, Interligne : Multiple 1,08 li

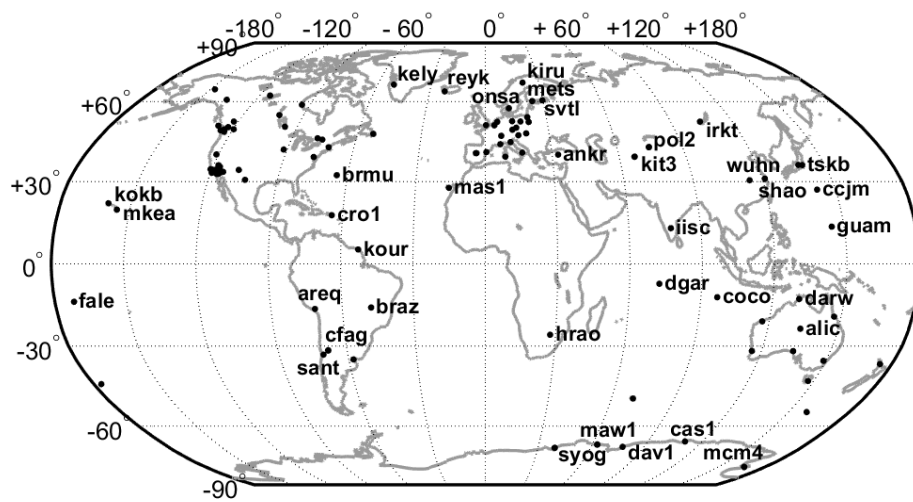


Figure 1: Map showing the 104 GPS stations used in this study. The stations discussed in the text [and the Annex](#) are identified by their 4-character ID.

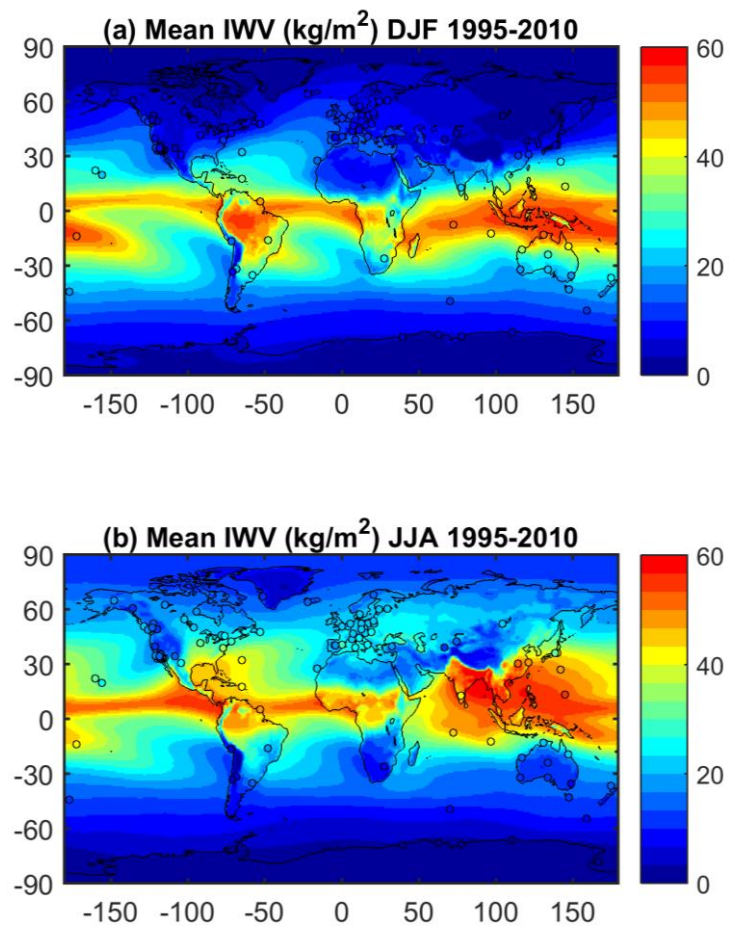


Figure 2: (a) Mean IWV for DJF 1995-2010 from ERA-Interim (shading) and GPS (filled circles), (b) same as (a) for JJA.

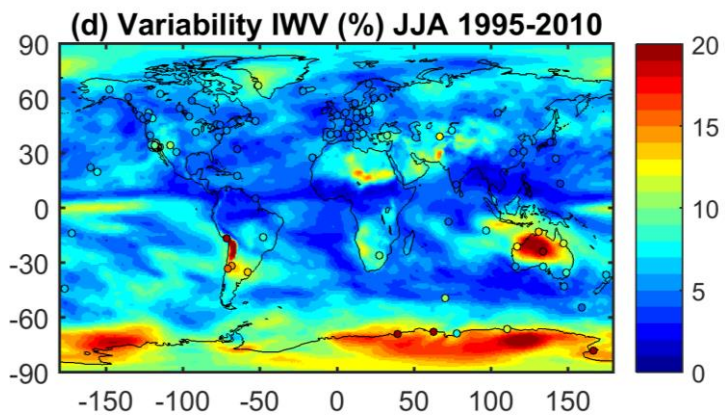
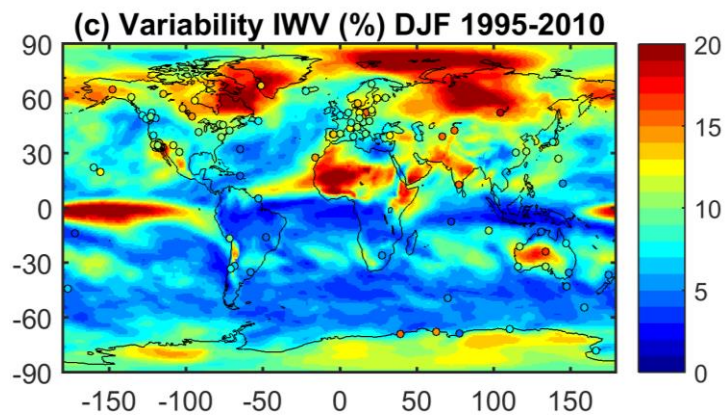


Figure 2 (continued): (c) Relative variability in % (standard deviation of the IWV series divided by its mean) for DJF 1995-2010, (d) Same as (c) for JJA.

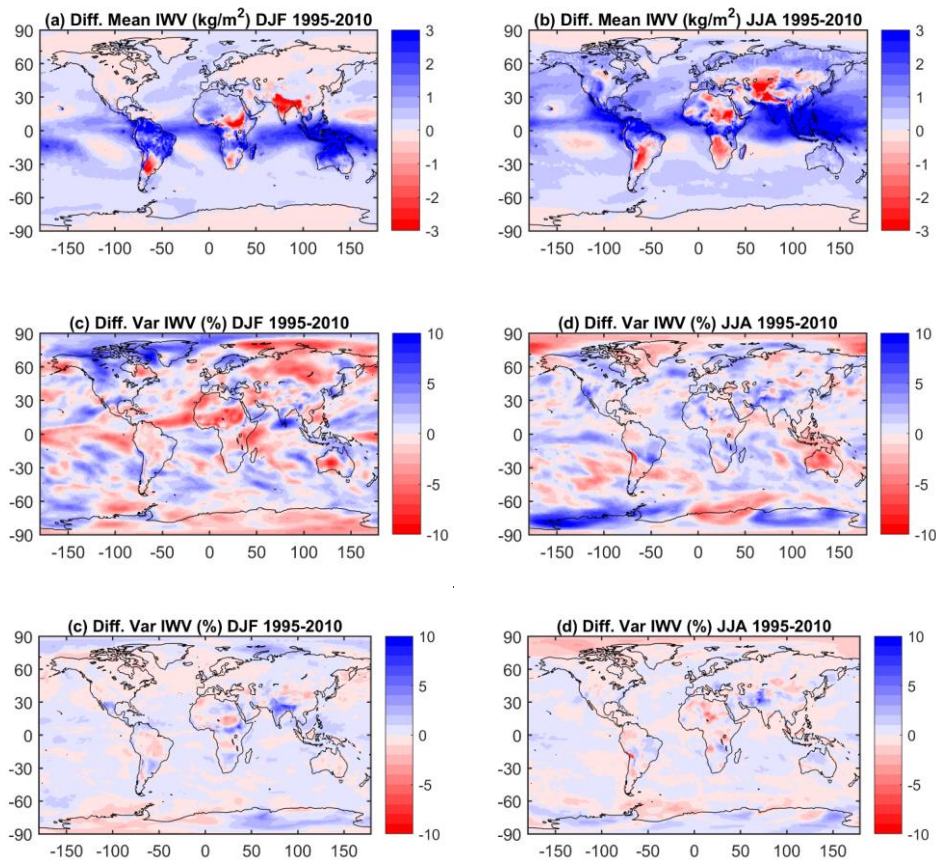
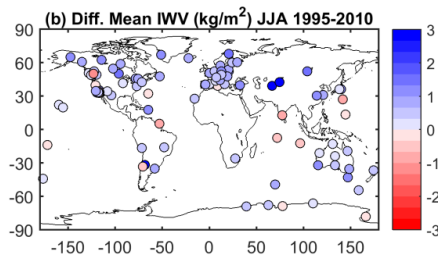
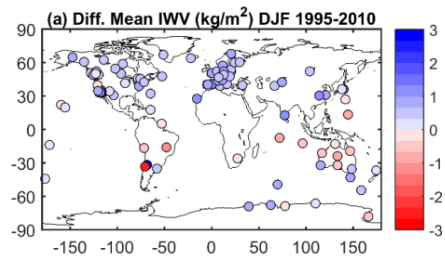
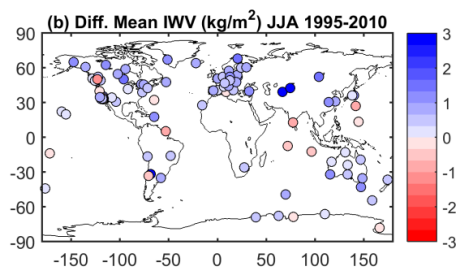
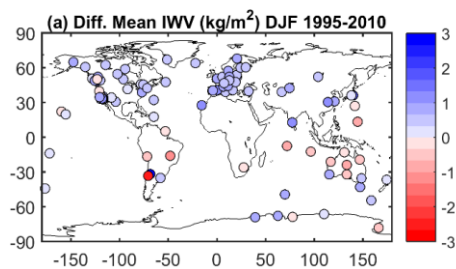


Figure 3: (a) Difference of mean IWV estimates (MERRA-2 minus ERA-Interim) for DJF 1995-2010. The global mean difference is 0.35 kg.m-2 (0.94 %) and the standard deviation of the difference is 0.32 kg.m-2 (1.56 %). (b) Same as (a) for JJA. The global mean difference is 0.56 kg.m-2 (1.66 %) and the standard deviation of the difference is 0.37 kg.m-2 (1.67 %). (c) Difference of relative variability estimates (MERRA-2 variability minus ERA-Interim variability) for DJF 1995-2010. The global mean difference is -0.01 % and the standard deviation of the difference is 0.26 %. (d) same as (c) for JJA. The global mean difference is 0.28 % and the standard deviation of the difference is 0.42 %.



Mis en forme : Interligne : simple

Mis en forme : Centré, Espace Avant : 0 pt, Interligne : simple, Position : Horizontal : Gauche, Par rapport à : Colonne, Vertical : En ligne, Par rapport à : Marge, Horizontal : 0 cm, Renvoi ligne automatique

Mis en forme : Police : Non Gras

Mis en forme : Police : Non Gras

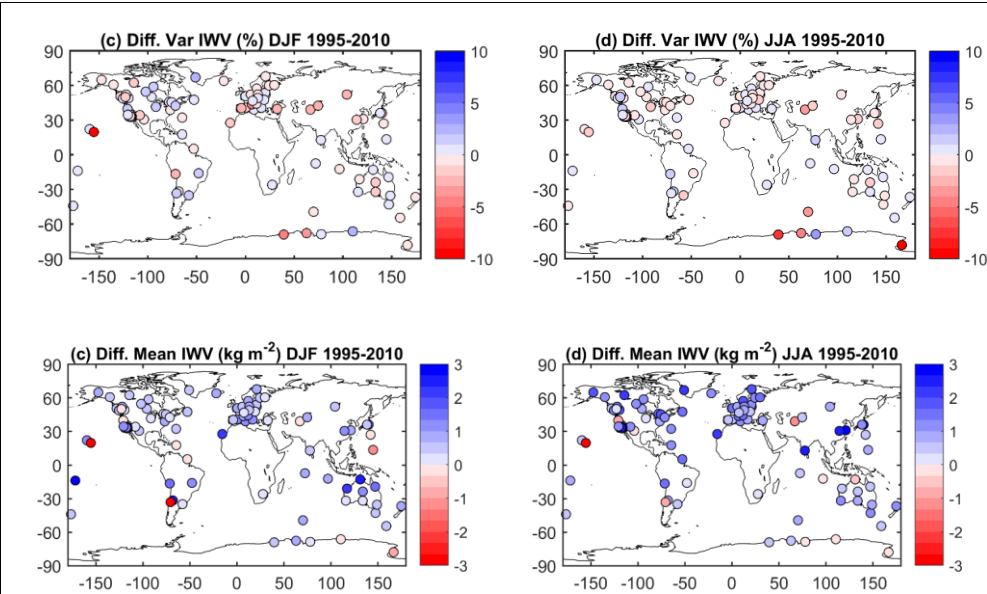
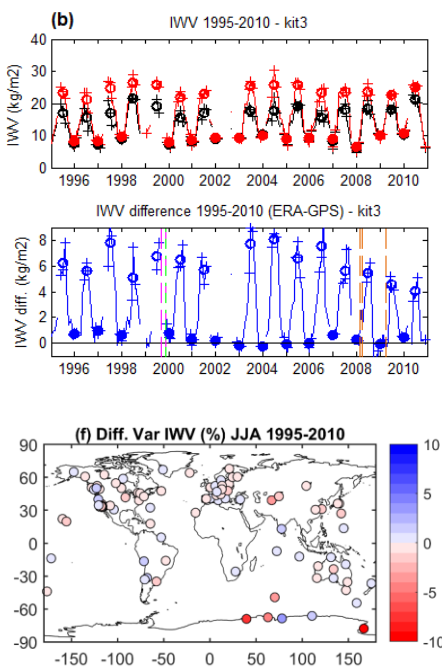
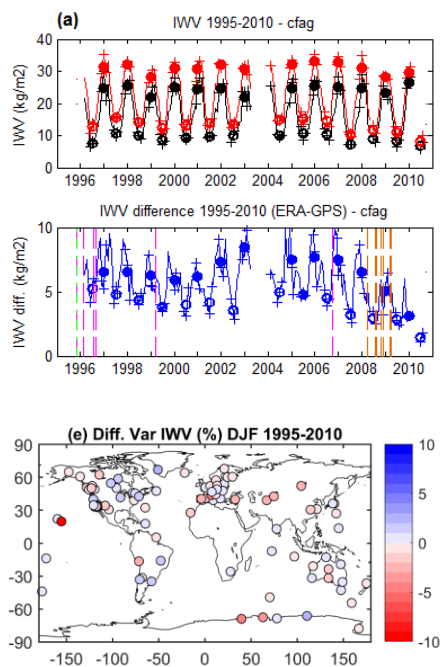


Figure 4: (a, b) Difference of mean IWV estimates (ERA-Interim minus GPS) for DJF and JJA 1995-2010; (c, d) same as (a, b) for MERRA-2 minus GPS. The monthly data were time-matched before seasonal means were computed.

Mis en forme : Centré, Espace Avant : 0 pt, Interligne : simple, Position :Horizontal : Gauche, Par rapport à : Colonne, Vertical : En ligne, Par rapport à : Marge, Horizontal : 0 cm, Renvoi ligne automatique

Mis en forme : Police :Non Gras

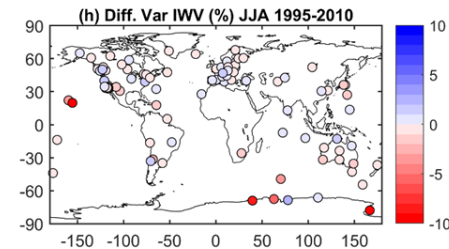
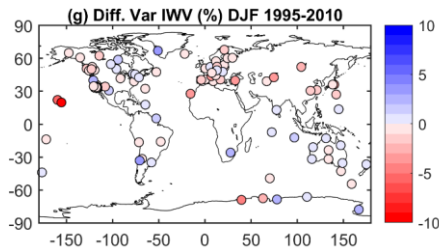
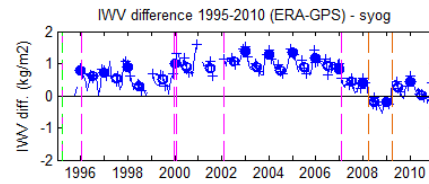
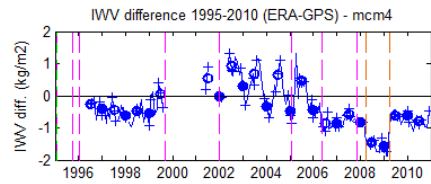
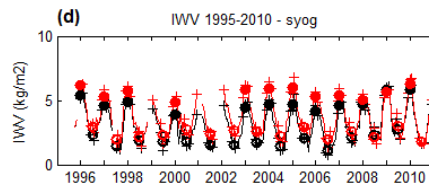
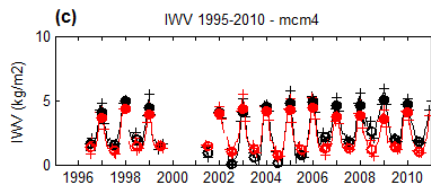
Mis en forme : Police :Non Gras



Mis en forme : Centré, Espace Avant : 0 pt, Interligne : simple, Position :Horizontal : Gauche, Par rapport à : Colonne, Vertical : En ligne, Par rapport à : Marge, Horizontal : 0 cm, Renvoi ligne automatique

Mis en forme : Police :Non Gras

Mis en forme : Police :Non Gras



Mis en forme : Centré, Espace Avant : 0 pt, Interligne : simple, Position :Horizontal : Gauche, Par rapport à : Colonne, Vertical : En ligne, Par rapport à : Marge, Horizontal : 0 cm, Renvoi ligne automatique

Mis en forme : Police :Non Gras

Mis en forme : Police :Non Gras

Figure 4 (continued): (e, f) Difference of relative standard deviations of IWV estimates (ERA-Interim std. minus GPS std.) for DJF and JJA 1995-2010; (g, h) same as (e, f) for MERRA-2 minus GPS. The monthly data were time-matched before seasonal means were computed.

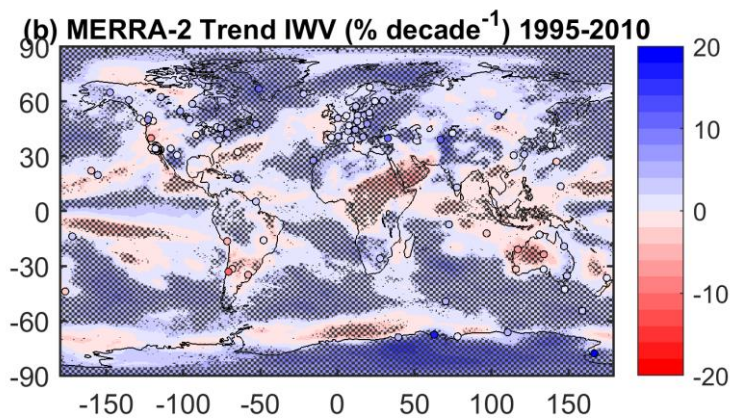
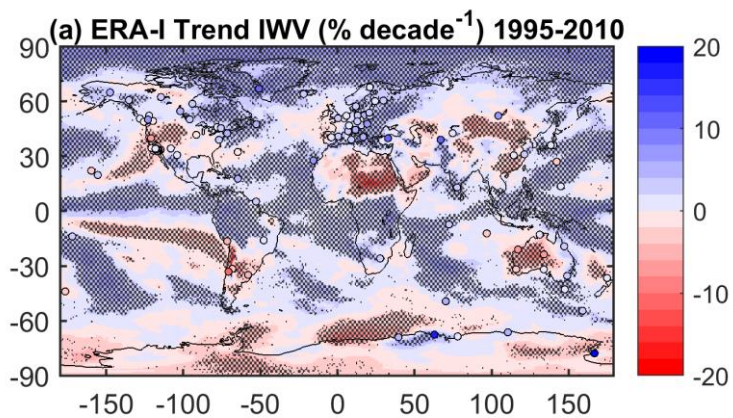


Figure 5: Time series of IWV from GPS (black) and ERAI (red), and IWV difference (blue) at stations (a) CFAG, (b) KIT3, (c) MCM4 and (d) SYOG. Filled circles show the DJF values and open circles the JJA values. Crosses show the individual months used in both seasons. Vertical dashed lines indicate GPS equipment changes (receiver in magenta, antenna in green) and GPS processing changes (in orange). **Note the change in vertical scales between figures.**

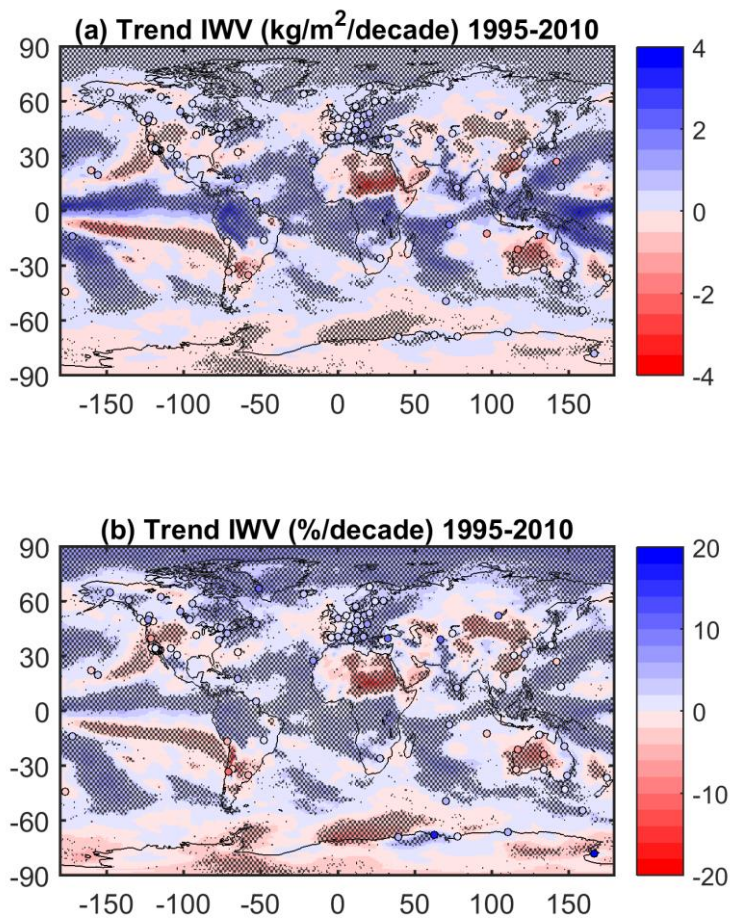


Figure 6: Absolute (a) and relative (b) Relative IWV trends (in % per decade) for the 1995-2010 period from ERA-Interim and GPS (stations marked as circles), and ERA-Interim (a), and MERRA-2 (b). The statistically significant trends from ERA-Interim and MERRA-2 are highlighted by stippling. Absolute trends are in kg.m^{-2} per decade and relative trends in % per decade.

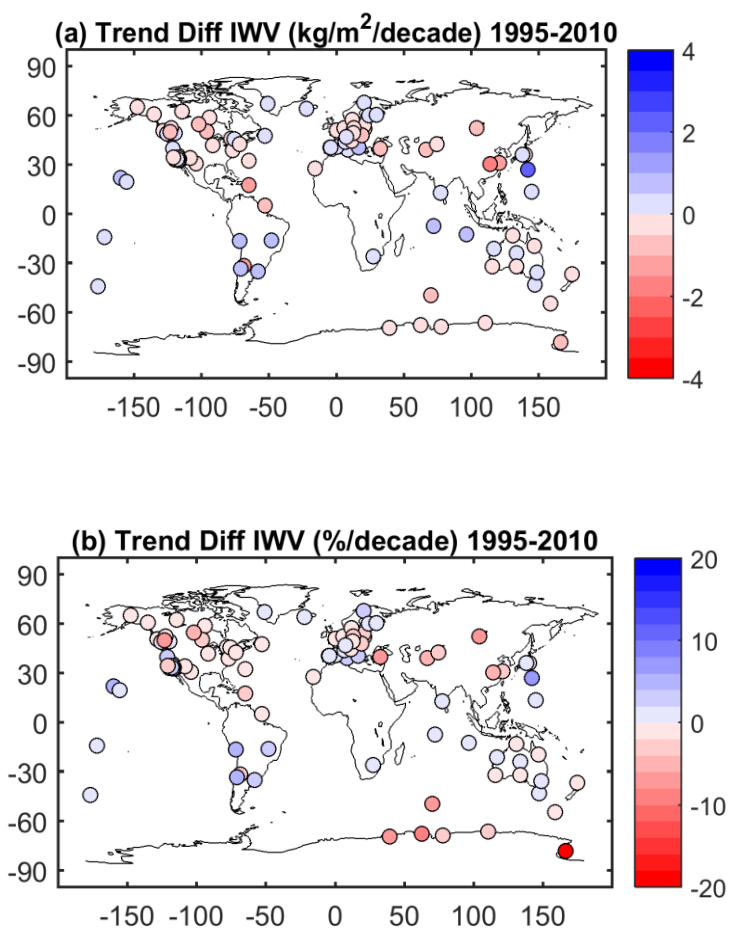


Figure 7: Difference of IWV trends (ERA-Interim minus GPS) for the 1995 to 2010 period, for time-matched series: (a) trends in $\text{kg}\cdot\text{m}^{-2}$ per decade and (b) relative trends in $\%$ per decade.

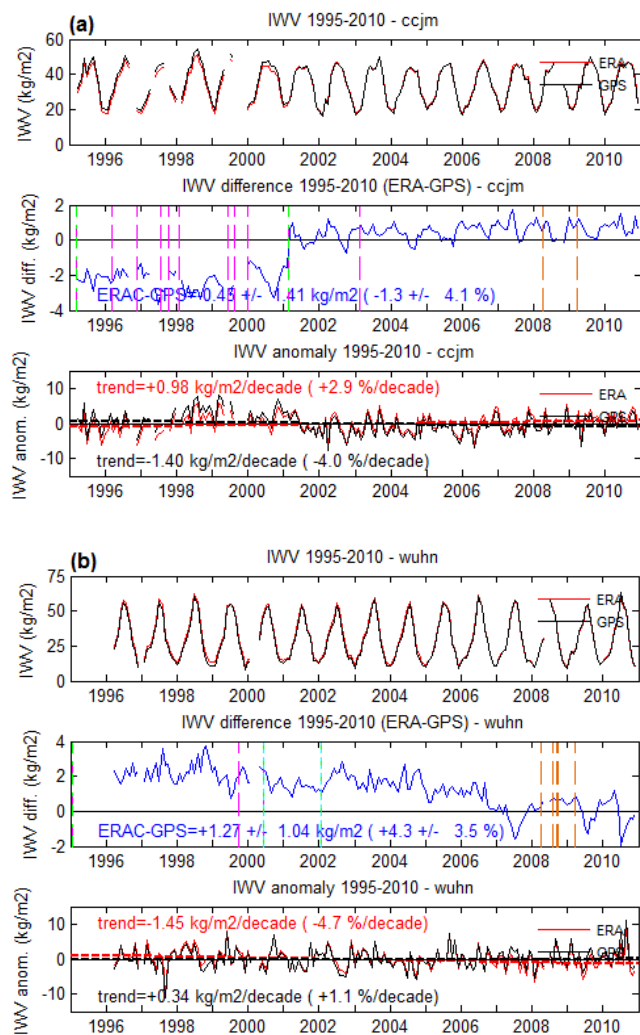


Figure 8: Examples of GPS time-series with inhomogeneities: (a) station CCJM and (b) WUHN. Upper plots show IWV for GPS (black) and ERA-Interim (red), middle plots show IWV difference (ERA-Interim minus GPS) and lower plots show monthly anomalies with their linear trend estimates (dashed lines).

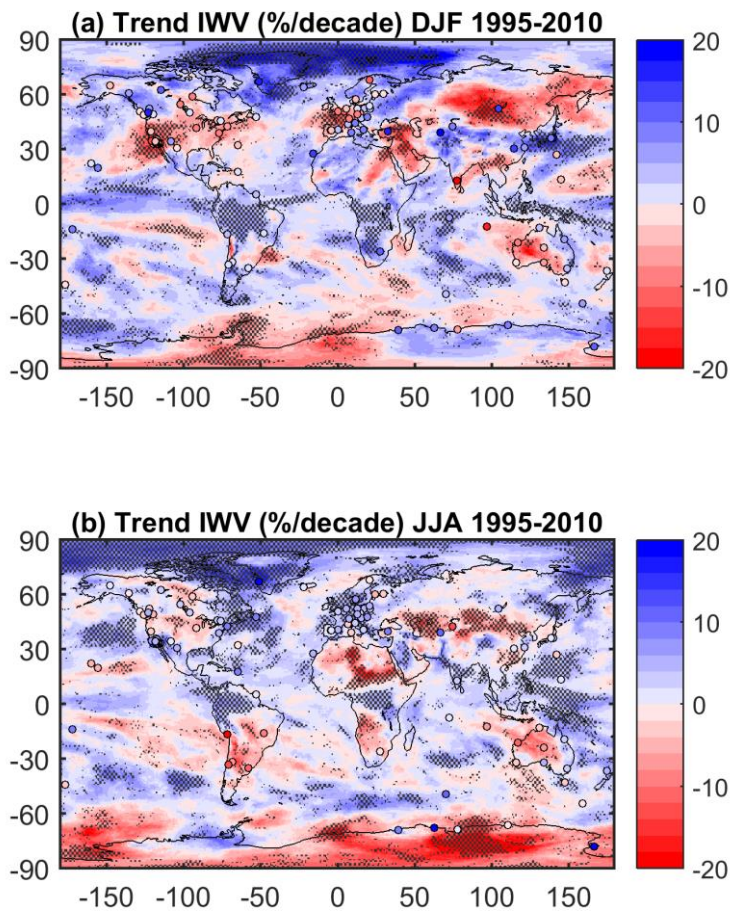


Figure 9

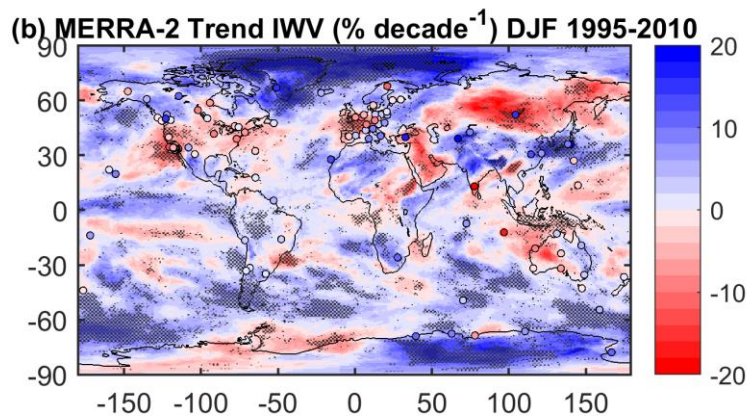
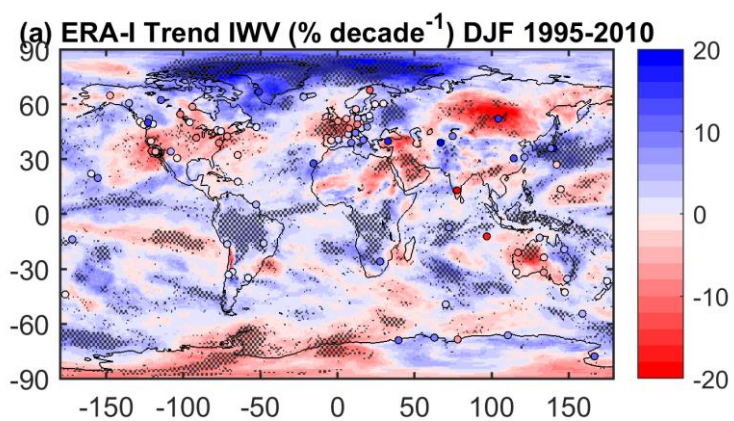
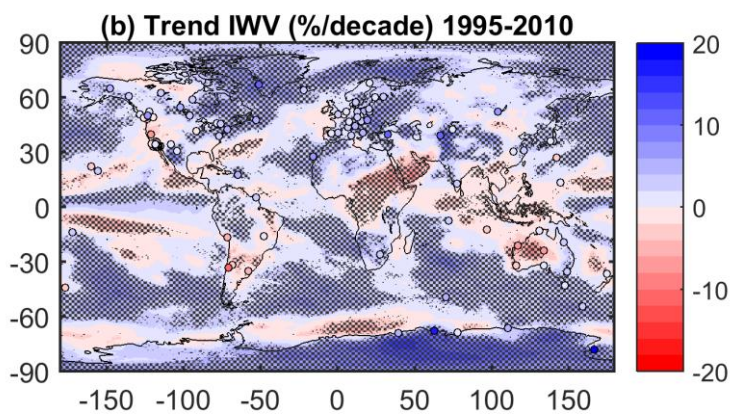
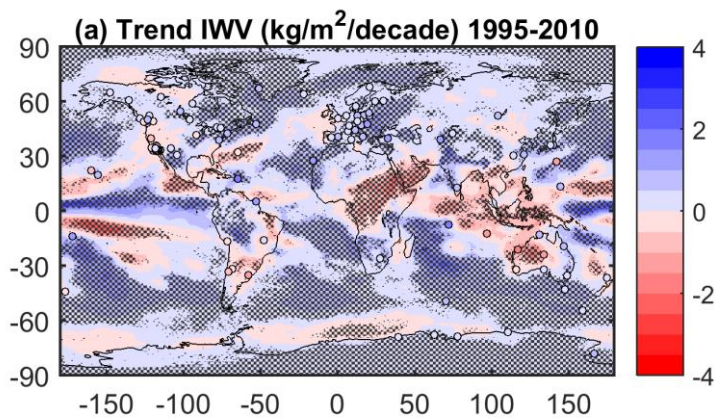


Figure 6: Seasonal IWV trends for the 1995-2010 period from ERA-Interim (shading) and GPS (filled circles) for DJF (a) and JJA (b). Same as (a) but for MERRA-2. The statistically significant trends from ERA-Interim the reanalyses are highlighted by stippling.



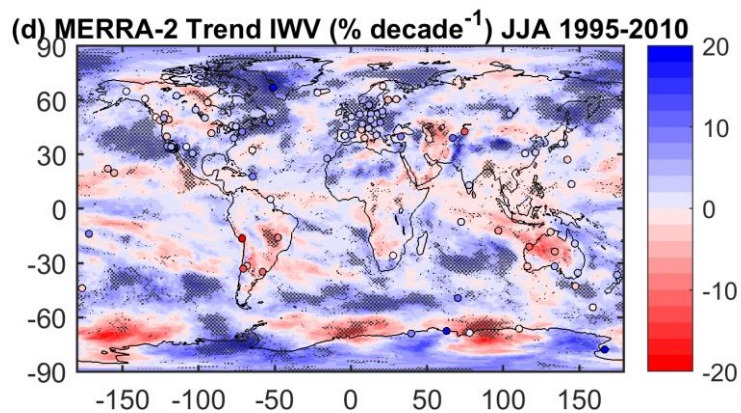
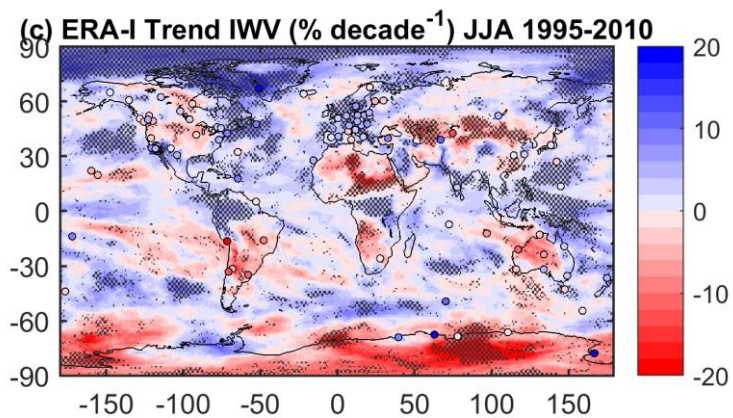
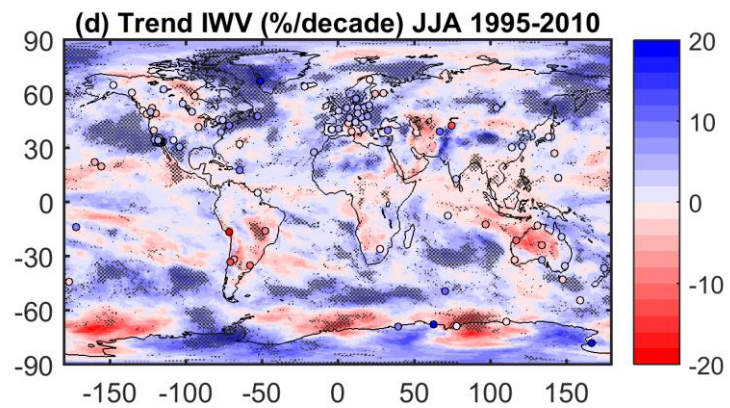
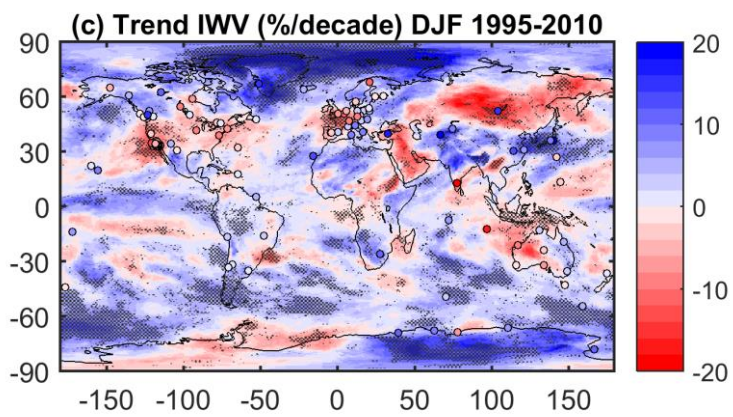


Figure 10: Absolute (continued): (c) Same as (a) and relative (b) trends in IWV in the MERRA-2 reanalysis but for the 1995-2010 period, JJA. (d) Same as (b) but for JJA. The statistically significant trends from the reanalyses are highlighted by stippling.

Mis en forme : Français (France)



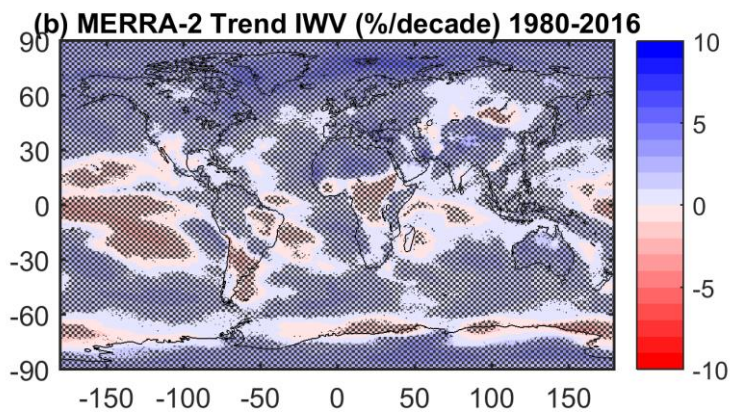
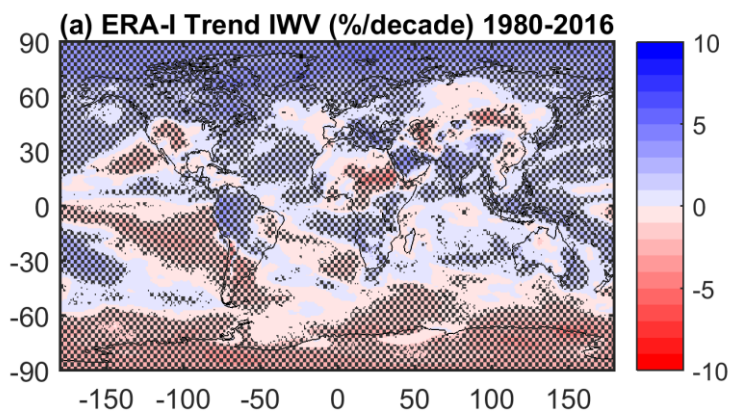


Figure 10 (continued): Relative trends in IWV in the MERRA-2 reanalysis for the 1995-2010 period for DJF (c) and JJA (d). The statistically significant trends are highlighted by stippling.

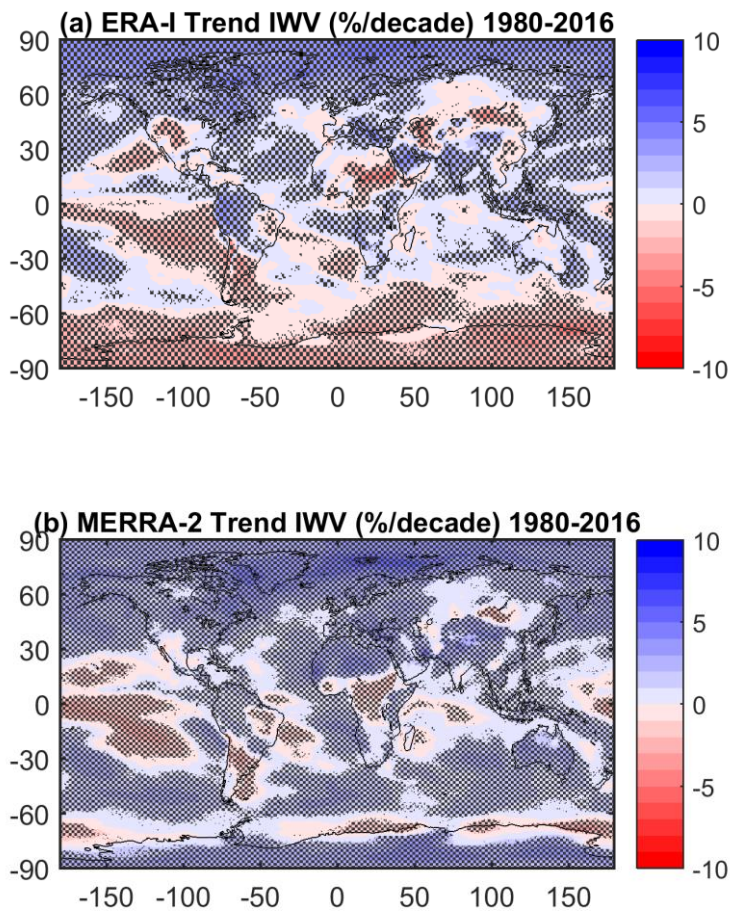


Figure 117: Monthly trends in IWV for the 1980-2016 period for: (a) ERA-Interim, (b) MERRA-2. The statistically significant trends are highlighted by stippling.

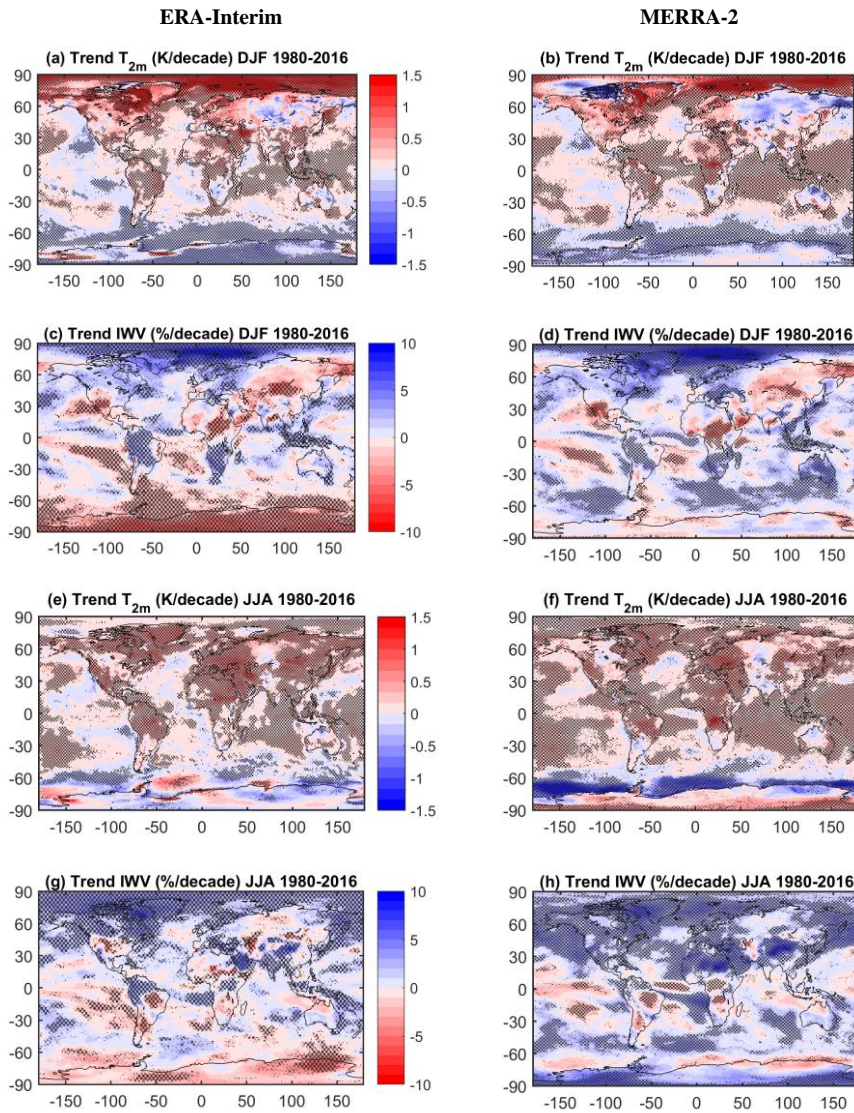


Figure 128: Seasonal trends in T2m and IWV for the 1980 to 2016 period for: (left) ERA-Interim and (right) MERRA-2.

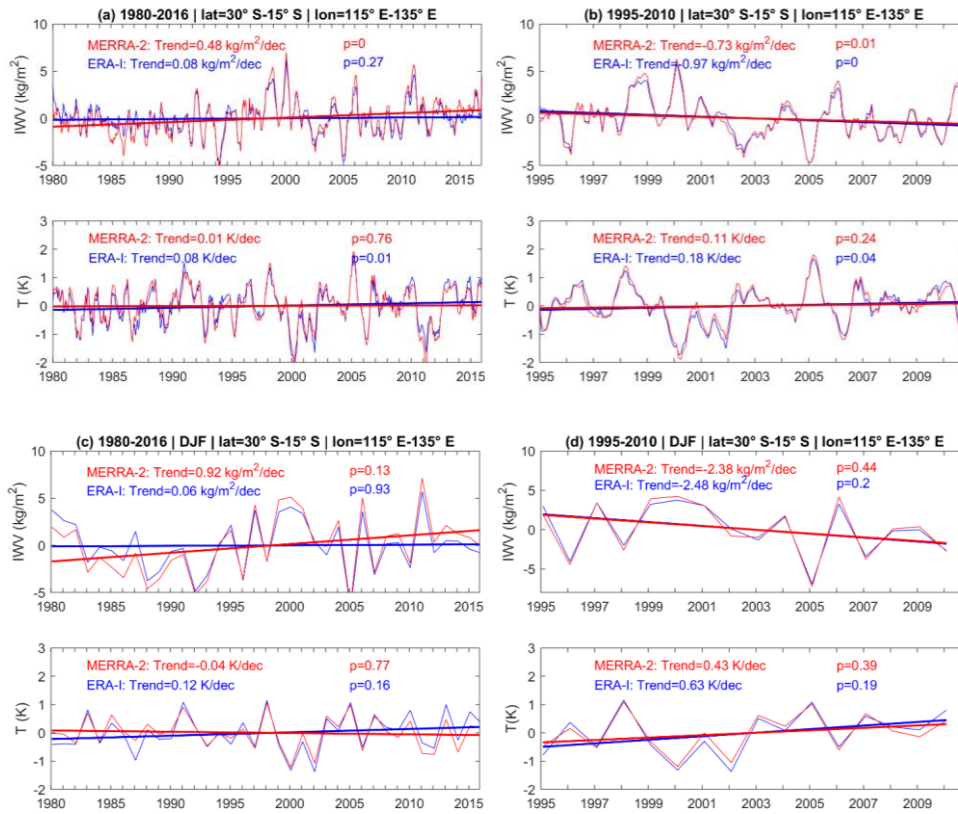
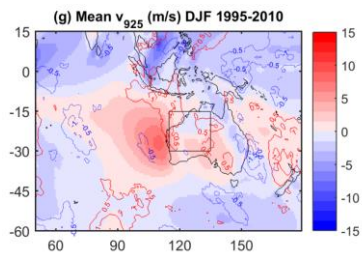
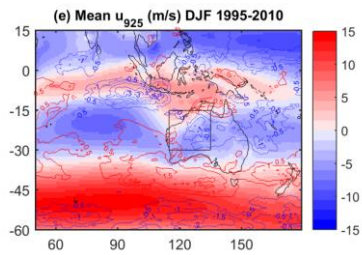
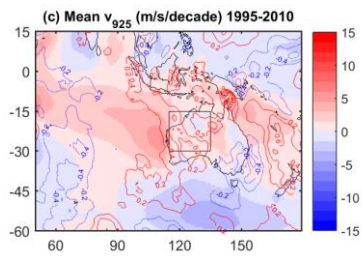
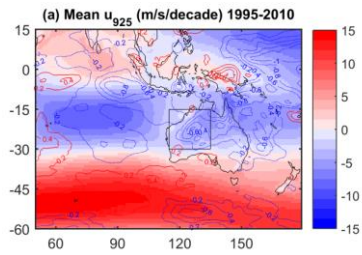


Figure 139: Temperature and IWV anomalies time series for a box over Western Australia (see Fig. 1414), using ERA-Interim (blue) and MERRA-2 (red) data, for: (a, c) the 1980 to 2016 period, (b, d) the 1995 to 2010 period, and (a, b) the monthly time series and (c, d) the DJF season.

ERA-Interim



MERRA-2

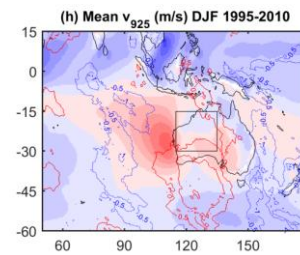
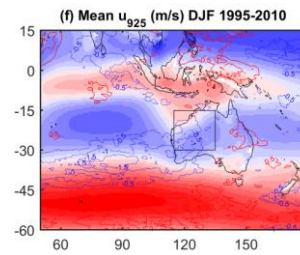
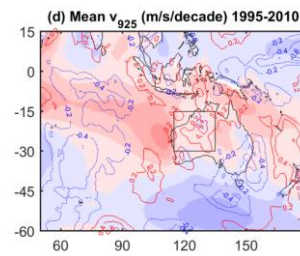
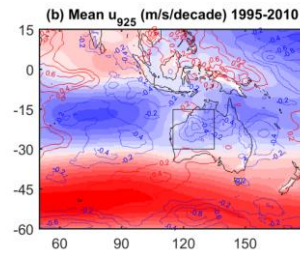


Figure 10: Zoom over Western Australia of the mean monthly and DJF fields and trends of the u and v wind components at 925 hPa (shaded) and their trends (contours). The area of focus (where IWV trends are most intense in ERA-Interim) is marked by a box.

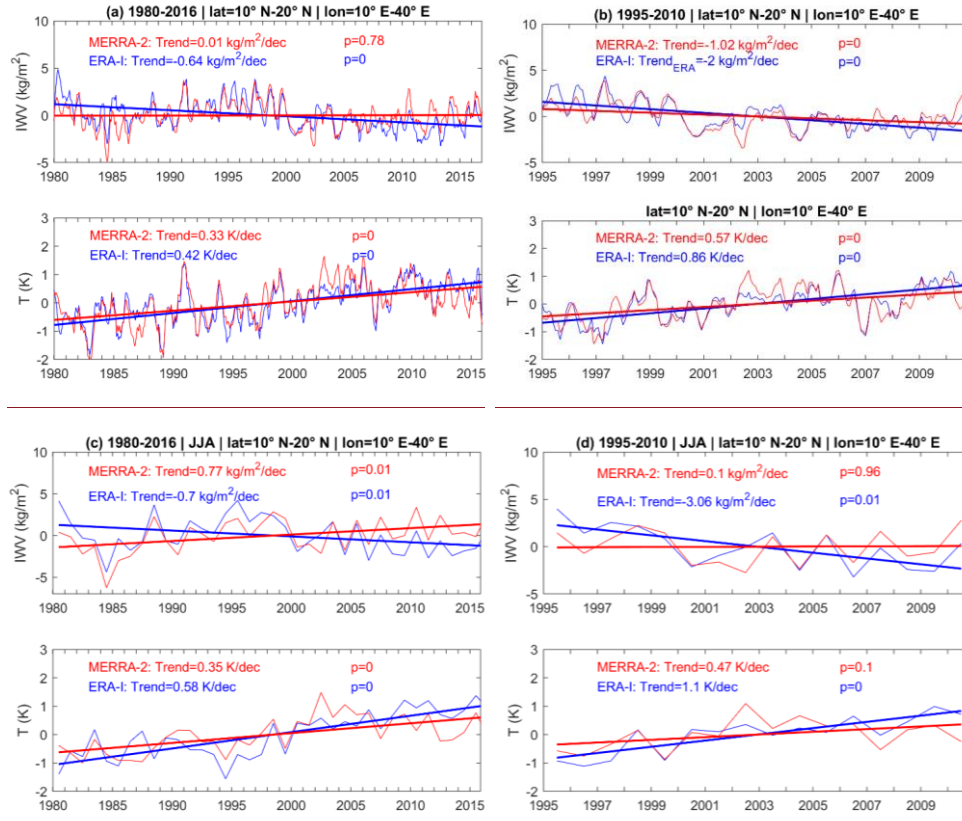
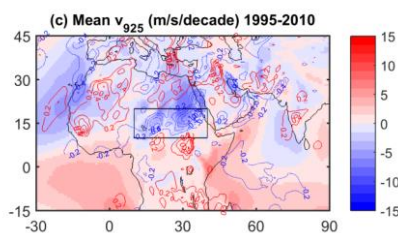
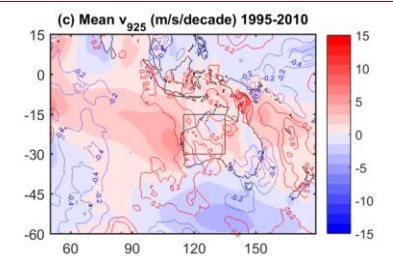
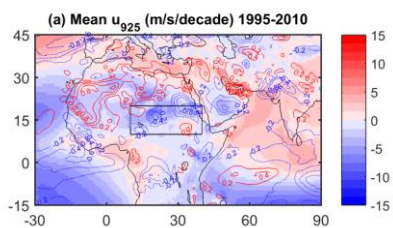
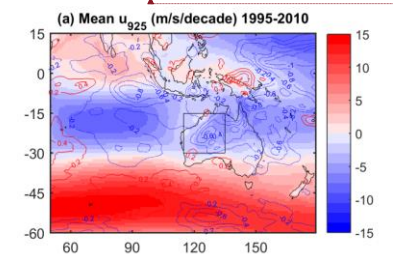
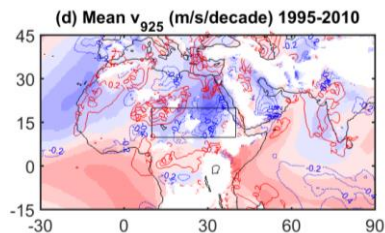
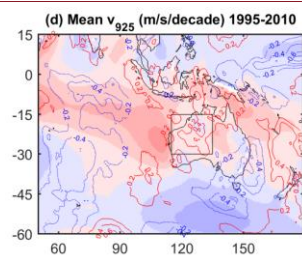
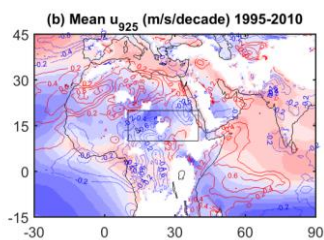
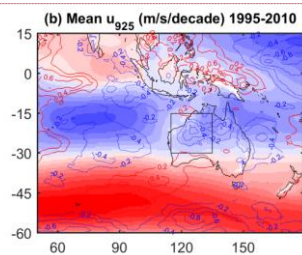


Figure 11: Temperature and IWV anomalies time series for a box over eastern Sahel (see Fig. 17), using ERA-Interim (blue) and MERRA-2 (red) data, for: (a, c) the 1980 to 2016 period, (b, d) the 1995 to 2010 period, and (a, b) the monthly time series and (c, d) the **DJFJJA** season.

ERA-Interim



MERRA-2



Mis en forme : Police :Gras

Tableau mis en forme

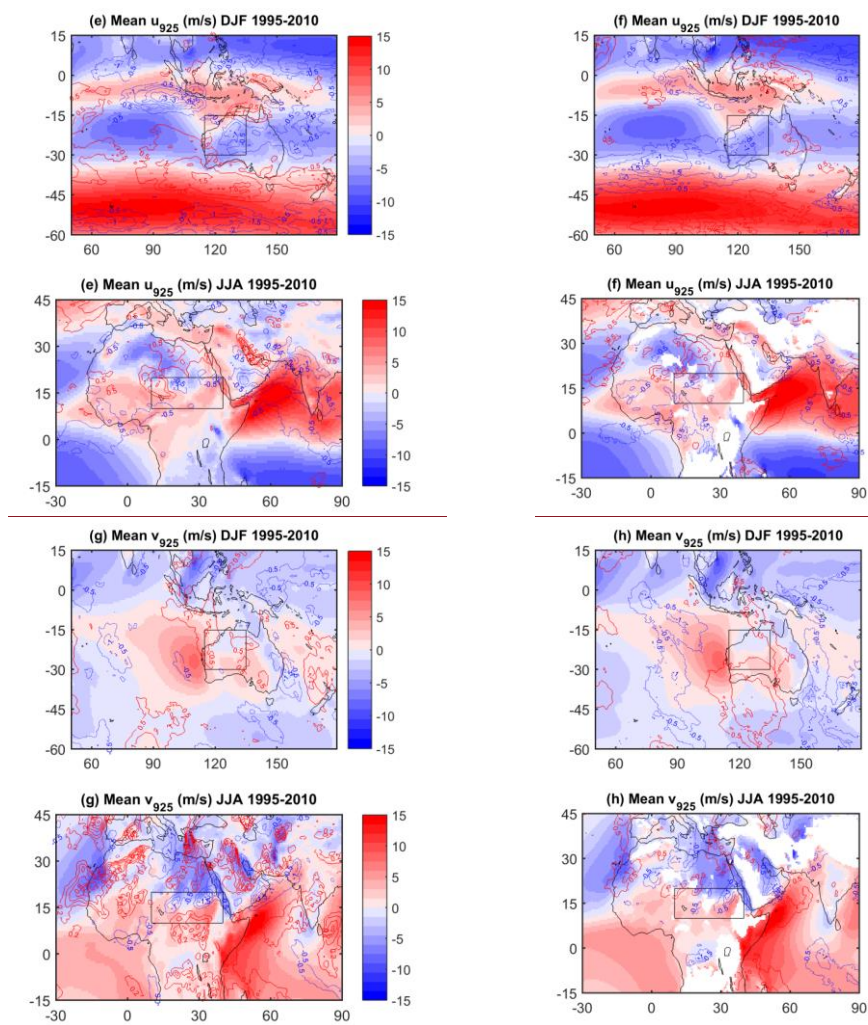
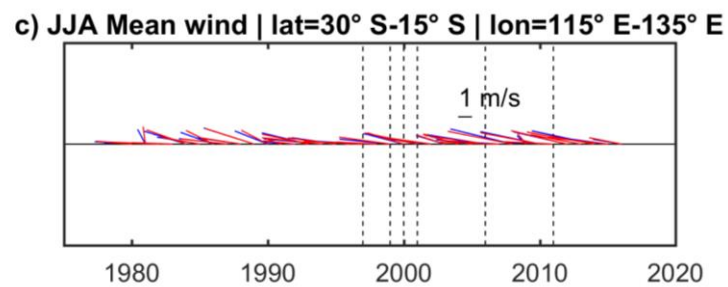
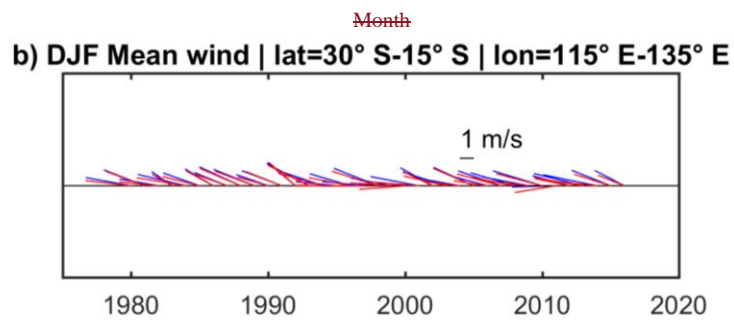
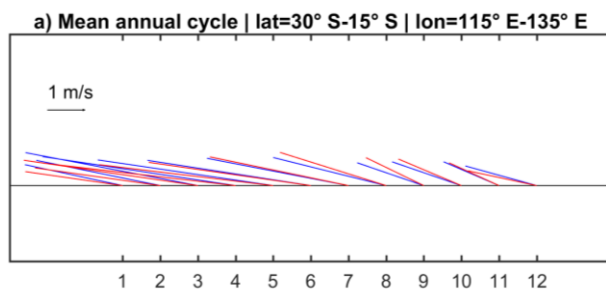


Figure 1412: Zoom over Western Australia/North Africa of the mean monthly and DJF/JJA fields and trends of the u and v wind components at 925 hPa (shaded) and their trends (contours). The area of focus (where IWV trends are most intense in ERA-Interim) is marked by a box.



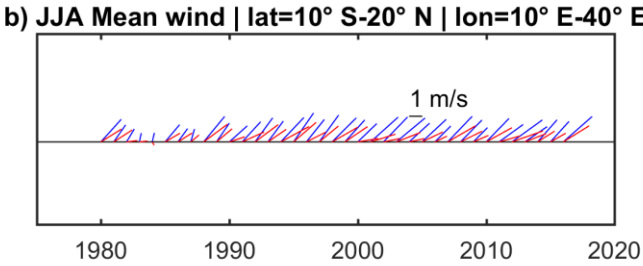
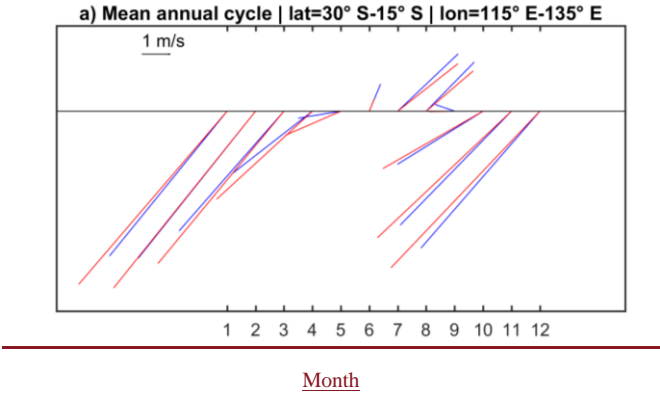
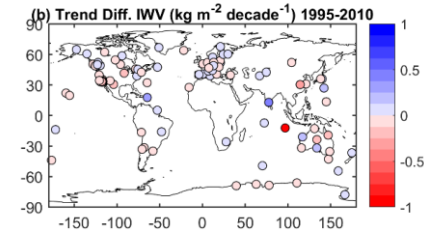
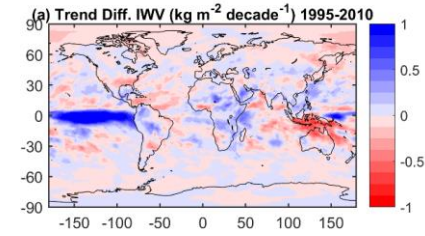
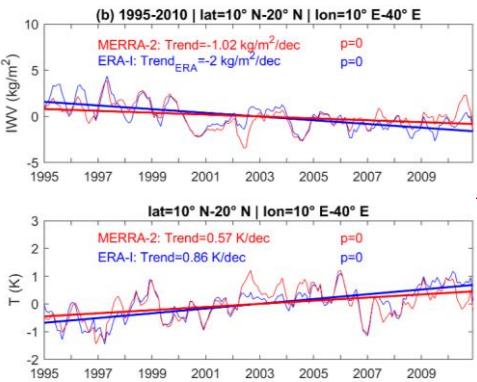
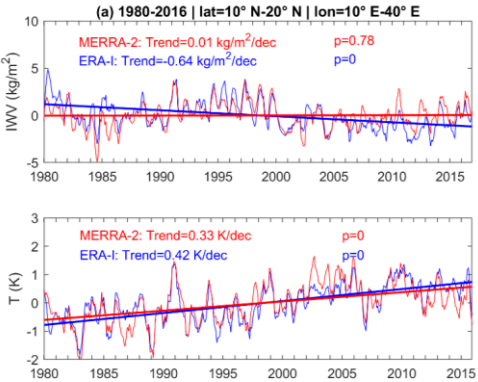


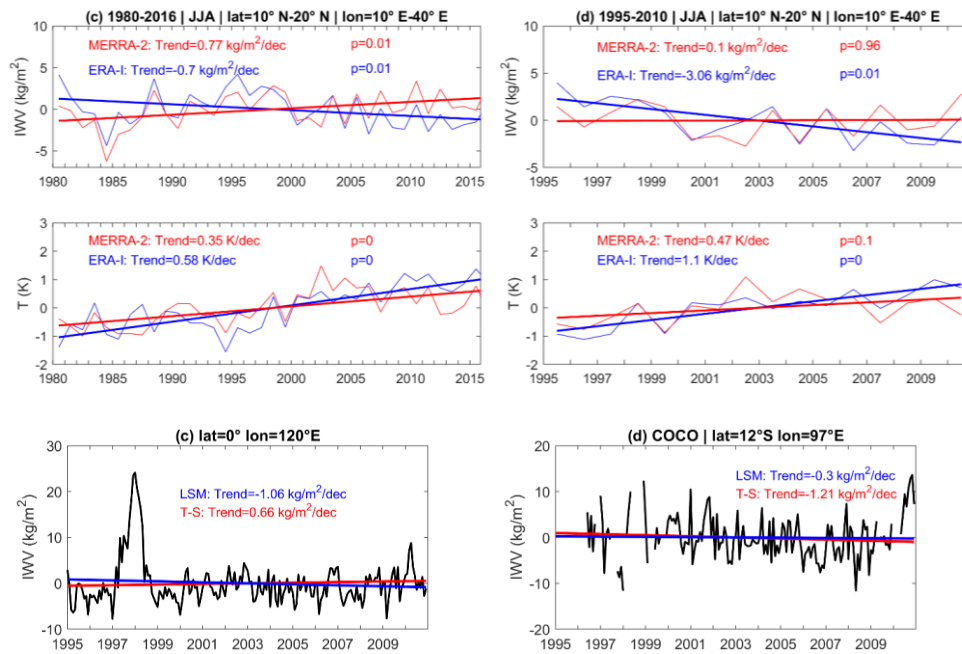
Figure 1513: Time series of mean wind vectors for a box over Western Australia Eastern Sahel (see Fig. 1415), using ERA-Interim (blue) and MERRA-2 (red) data, for the 1980 2016 period: mean annual cycle (a), and the monthly time series for the DJF and JJA seasons (b, c).



Mis en forme : Justifié, Interligne : 1,5 ligne

Tableau mis en forme

Mis en forme : Justifié, Paragraphes solidaires

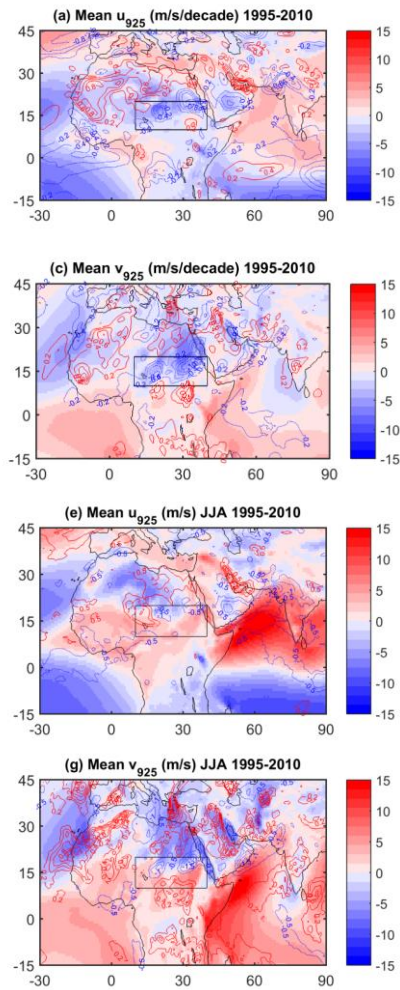


Mis en forme : Justifié, Paragraphes solidaires

Figure A1: (a) Trend differences between two methods of computing trends (Theil Sen minus the Least Squares method) for the ERA-Interim data used in the paper. The root mean square of the difference is $0.20 \text{ kg.m}^{-2}.\text{decade}^{-1}$. (b) Same as (a), but for the GPS data at 104 stations. The root mean square of the difference is $0.14 \text{ kg.m}^{-2}.\text{decade}^{-1}$. (c) Time series of IWV anomaly in ERA-Interim at a point of large difference between methods in the tropical Pacific ocean with superposed linear trends. (d) Time series of IWV anomaly at the COCO GPS site with superposed linear trends.

Figure 16: Temperature and IWV anomalies time series for a box over eastern Sahel (see Fig. 17), using ERA-Interim (blue) and MERRA-2 (red) data, for: (a, c) the 1980 to 2016 period, (b, d) the 1995 to 2010 period, and (a, b) the monthly time series and (c, d) the JJA season.

ERA-Interim



MERRA-2

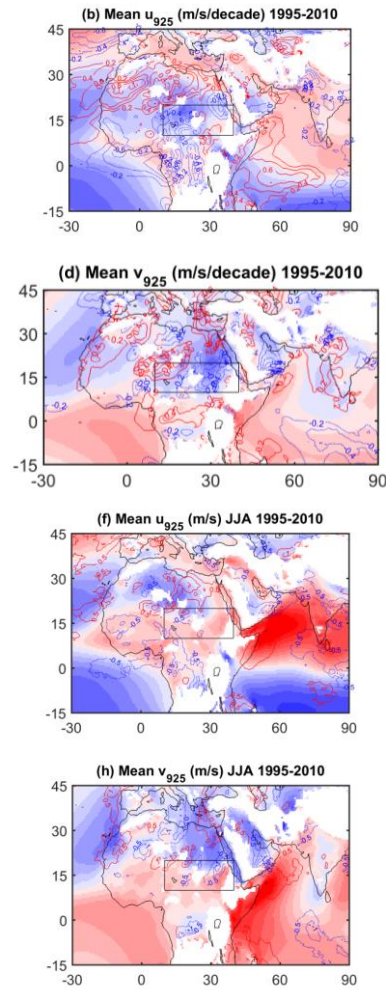


Figure 17: Zoom over North Africa of the mean monthly and JJA fields and trends of the u - and v -wind components at 925 hPa (shaded) and their trends (contours). The area of focus (where IWV trends are most intense in ERA-Interim) is marked by a box.

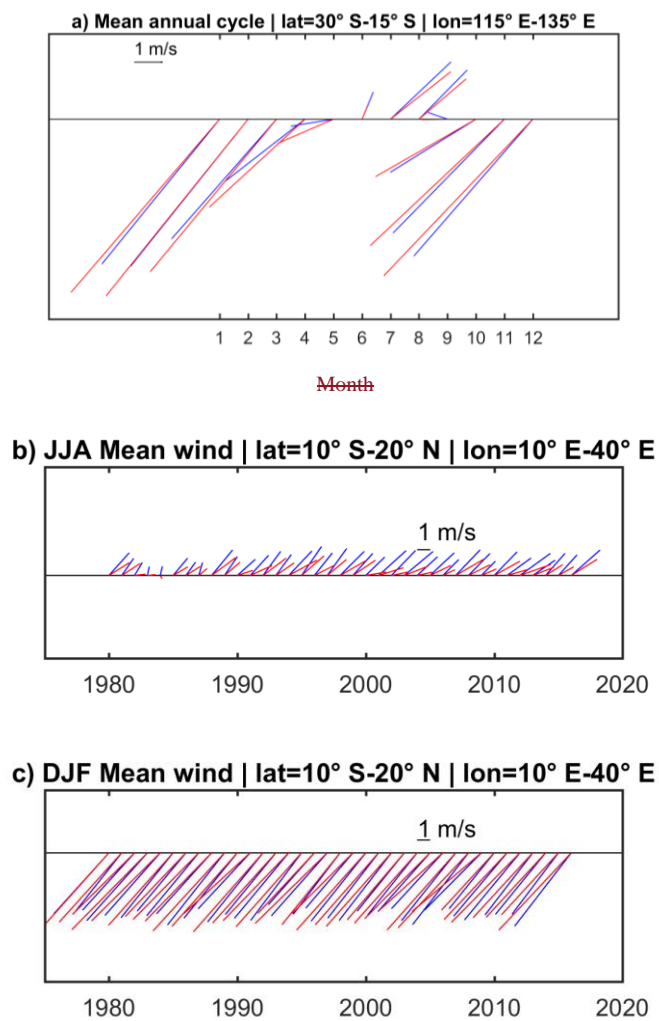


Figure 18: Time-series of mean-wind-vectors for a box over Eastern-Sahel (see Fig. 17), using ERA-Interim (blue) and MERRA-2 (red) data, for the 1980-2016 period: mean annual cycle (a), and the monthly time-series for the JJA and DJF seasons (b, c).

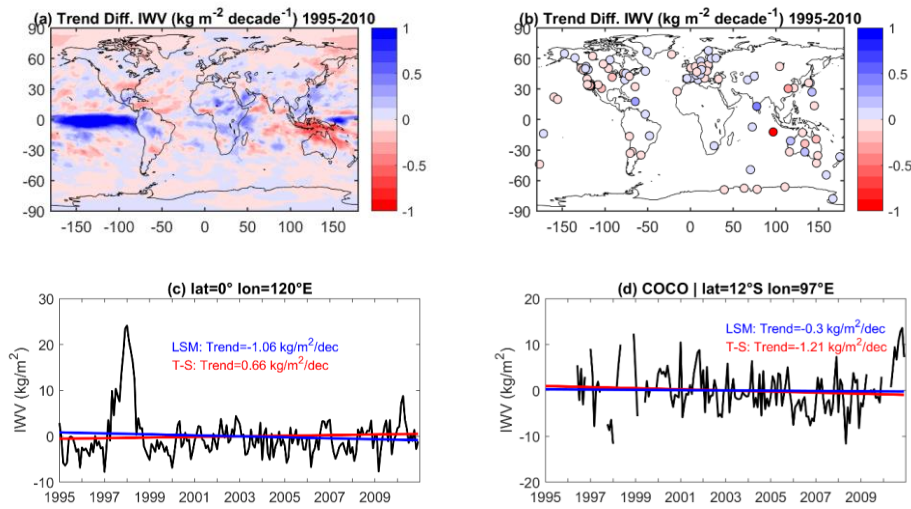


Figure A3: (a) Trend differences between two methods of computing trends (Theil Sen minus the Least Squares method) for the ERA-Interim data used in the paper. The root mean square of the difference is $0.20 \text{ kg m}^{-2} \text{decade}^{-1}$. (b) Same as (a), but for the GPS data at 104 stations. The root mean square of the difference is $0.14 \text{ kg m}^{-2} \text{decade}^{-1}$. (c) Time series of IWV anomaly in ERA-Interim at a point of large difference between methods in the tropical Pacific ocean with superposed linear trends. (d) Time series of IWV anomaly at the COCO GPS site with superposed linear trends.

Table B1: Stations with most intense trend differences (ERA1 – GPS) computed from time-matched GPS and ERA-Interim IWV series.

	<u>Full time series</u>	<u>DJF</u>	<u>JJA</u>
<u>Tr.diff < -1 kg.m⁻².decade⁻¹</u>	<u>WUHN, CRO1, CFAG, SHAO</u>	<u>WUHN, PIN1</u>	<u>WUHN, SHAO, CRO1, CFAG, KOUR, WSLR</u>
<u>Tr.diff > 1 kg.m⁻².decade⁻¹</u>	<u>CCJM</u>	<u>CCJM, DARW, GUAM, LPGS, COCO, SANT</u>	<u>CCJM, POL2</u>
<u>Tr.diff < -7 %.decade⁻¹ (*)</u>	<u>MCM4, MAW1, PIN1</u>	<u>IRKT, POL2, PIN1, WUHN, YELL, WSLR</u>	<u>MCM4, MAW1, SYOG</u>
<u>Tr.diff > 7 %.decade⁻¹ (*)</u>	<u>CCJM</u>	<u>CCJM, KIRU</u>	<u>AREQ</u>

Mis en forme : Gauche, Espace Après : 8 pt, Interligne : Multiple 1,08 li

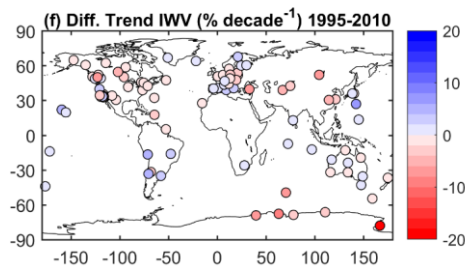
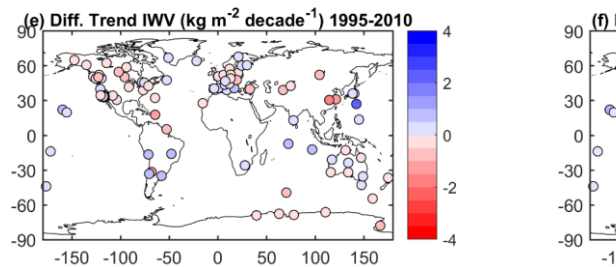
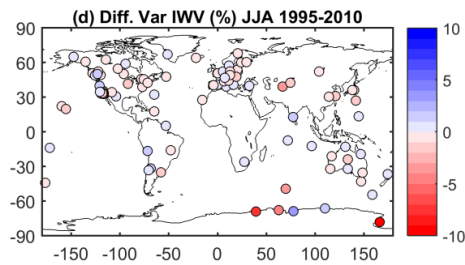
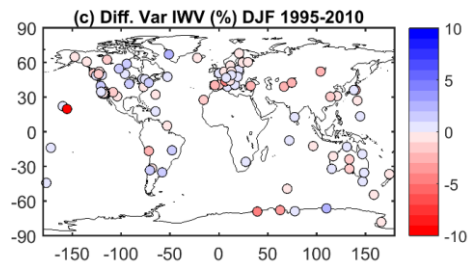
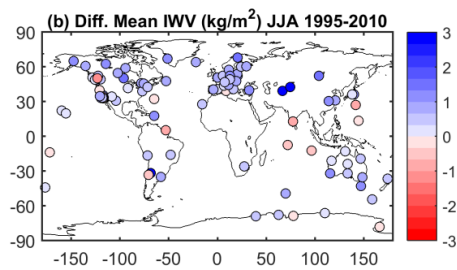
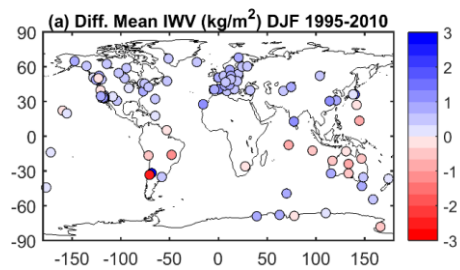


Figure B1: (a) Difference of mean IWV estimates (ERA-Interim minus GPS) for DJF 1995-2010 from time-matched IWV series, (b) same as (a) for JJA, (c) difference of relative variability estimates (ERA-Interim variability minus GPS variability) for DJF 1995-2010 from time-matched IWV series, (d) same as (c) for JJA, (e) difference of trend estimates (ERA-Interim minus GPS) for 1995-2010 from time-matched IWV series, (f) same as (e) for relative trends.

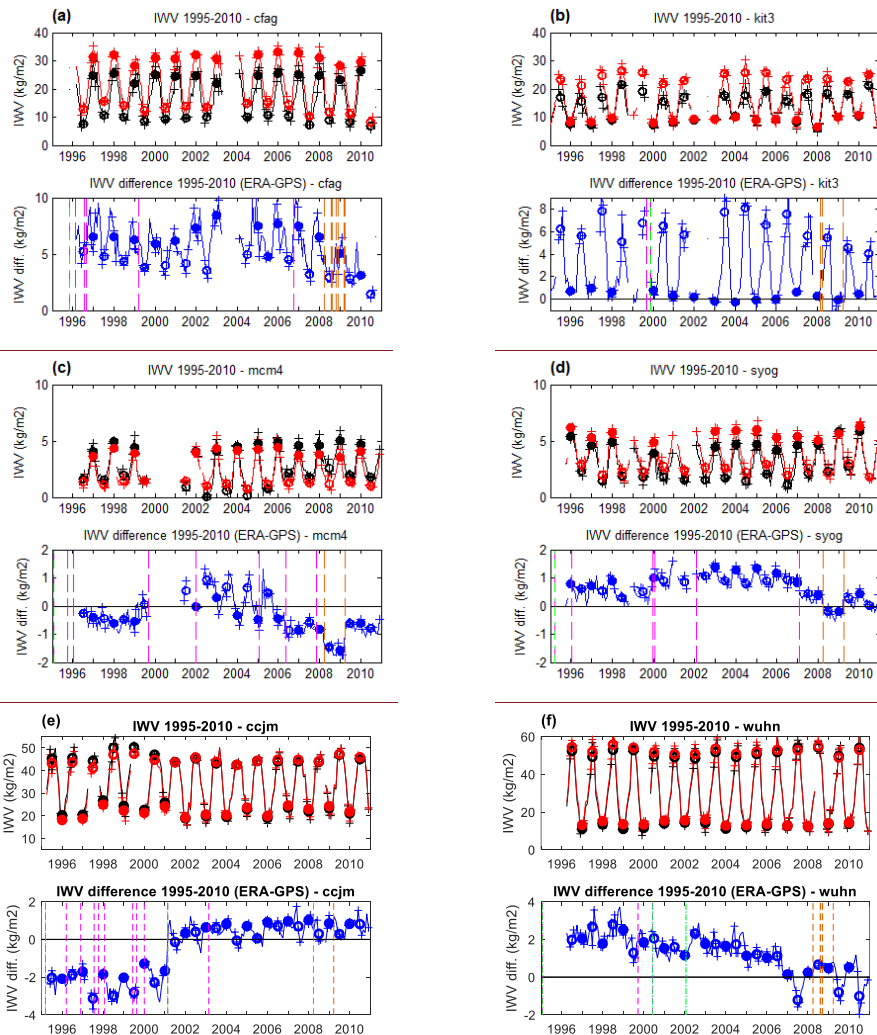


Figure B2: Time series of IWV from GPS (black) and ERAI (red), and IWV difference (blue) at stations (a) CFAG, (b) KIT3, (c) MCM4, (d) SYOG, (e) CCJM, and (f) WUHN. Filled circles show DJF values and open circles JJA values. Crosses show individual

Mis en forme : Légende

months used in both seasons. Vertical dashed lines indicate GPS equipment changes (receiver in magenta, antenna in green) and GPS processing changes (in orange). Note the change in vertical scales between figures.